Supporting information

Surface Inclusion of Cucurbit[7]uril-Based Supramolecular Complexes

Carina Santos Hurtado,[a‡] Guillaume Bastien,[a‡] Doroteja Lončarić,[a,b] Martin Dračínský,[a] Ivana Císařová,[c] Eric Masson,*[d] and Jiří Kaleta*[a]

[a] *Institute of Organic Chemistry and Biochemistry of the Czech Academy of Sciences, Flemingovo nám. 2, 160 00 Prague 6, Czech Republic*
[b] *Department of Organic Chemistry, Faculty of Science, Charles University in Prague, Hlavova 2030, 12840 Prague 2, Czech Republic*
[c] *Department of Inorganic Chemistry, Faculty of Science, Charles University in Prague, Hlavova 2030, 128 40 Prague 2, Czech Republic*
[d] *Department of Chemistry and Biochemistry, Ohio University, Athens, Ohio 45701, United States.*

Table of Contents

1. General Information

Materials. All reactions were performed under nitrogen atmosphere with dry solvents freshly distilled under anhydrous conditions unless otherwise stated. All of the starting material used for synthesis of guests was purchased from abcr (Karlsruhe, Germany) and Sigma-Aldrich (Prague, Czech Republic) and used without further purification. Cucurbit[7]uril (**CB[7]**) was prepared using known procedures.[1] The apparent molar mass of CB[7] was determined by measuring ^{1}H NMR spectrum with *p*-toluidine hydrochloride as an internal standard. Solvents used in preparation of samples for NMR measurements were purchased from Eurisotop. Deuterated dimethyl sulfoxide (DMSO-d_6) was distilled over calcium hydride as needed. Yields refer to isolated, chromatographically and spectroscopically homogenous materials.

Procedures. Analytical thin-layer chromatography (TLC) was performed using precoated TLC aluminum sheets (Silica gel 60 F254). TLC spots were visualized using UV light (254 nm). Column chromatography was performed using silica gel (high purity grade, pore size 60 Å, 70–230 mesh). The volume/volume (v/v) ratios of solvents were used to prepare mobile phases for column chromatographies.

Nuclear Magnetic Resonance (NMR) Spectroscopy. Characterization of prepared compounds by NMR was carried out using a Bruker Avance III^{TM} HD 400MHz Prodigy spectrometer. ^{1}H NMR titration experiments were carried out using a Bruker Avance II^{TM} 500MHz and JEOL JNM-EZCR 500 MHz spectrometers. Chemical shifts in ^{1}H and ^{13}C spectra are reported in ppm on the δ scale relative to $CHCl_3$ (δ = 7.26 ppm for ^{1}H and δ = 77.16 ppm for ^{13}C), DMSO-d_6 (δ = 2.50 ppm for ^{1}H, and δ = 39.5 ppm for ^{13}C) and MeCN-d_3 (δ = 1.94 ppm for ^{1}H and δ = 118.3 ppm for ^{13}C) as internal references. Coupling constants (*J*) are reported in hertz (Hz). Standard abbreviations were used to indicate multiplicity: s = singlet, d = doublet, t = triplet, q = quartet, m = multiplet, dd = doublet of doublets. Structural assignments were made with additional information from APT, COSY, HSQC, and HMBC experiments.

Solid-State NMR. High-resolution ^{31}P and ^{13}C solid-state NMR spectra were obtained using a JEOL ECZ600R spectrometer operating at 243.0 MHz for ^{31}P, 150.9 MHz for ^{13}C, and 600.2 MHz for ^{1}H. The samples were packed into 3.2 mm magic-angle spinning rotors (MAS) and the measurements were taken at the MAS rates of 18 kHz. Phosphorus and carbon spectra were measured using cross polarization (CP); the phosphorus spectra were also measured using the single-pulse experiment (no CP, direct excitation of ^{31}P). The ^{13}C chemical shifts were referenced to crystalline DSS as a secondary reference (δ = 0.0 ppm for CH_3 carbon). The phosphorus spectra were referenced against $(NH_4)_2HPO_4$ (δ = 1.37 ppm). A ramped-amplitude shaped pulse was used during cross-polarization. The contact time for CP was 5 ms for ^{13}C and ^{31}P. The relaxation delays were estimated from ^{1}H saturation recovery experiments and ranged from 0.5 s to 1.5 s.

Melting Points. Melting points were measured on Stuart SMP 3 melting point apparatus and reported data are uncorrected.

Mass Spectrometry. High-resolution mass spectra (HRMS) using electrospray ionization (ESI) or atmospheric pressure chemical ionization (APCI) were obtained on ORBITRAP XL (Thermo). MALDI experiments were performed on Bruker Ultraflextreme. EI and CI spectra were recorded using Waters or Agilent 7250 GC/Q-TOF instruments.

Single Crystal X-Ray Diffraction. The diffraction data of single crystals of **6**, **8** and **10** were obtained on Bruker D8 VENTURE Kappa Duo PHOTONIII by IμS micro-focus sealed tube MoKα (λ= 0.71073Å) at 120K temperature of the crystal preserved by Cryostream Cooler 800. The structures were solved by direct methods (XT)[2] and refined by full matrix least squares based on F^2 (SHELXL2019).[3] The hydrogen atoms on carbon were fixed into idealized positions (riding model) and assigned temperature factors either $H_{iso}(H) = 1.2\ U_{eq}$(pivot atom).

Compounds **6** and **8** crystallized in non-centrosymmetric, achiral space groups. The absolute configurations of both structures[4] were determined based on the anomalous dispersion of bromine atoms. The resulting absolute structure parameters were −0.009(5) for compound **6** and −0.0014(15) for compound **8**.

The crystal structure of compound **10** included disordered methanol solvent within the unit cell. To enhance the accuracy of the model for the principal molecule, the SQUEEZE procedure implemented in PLATON[5] was employed to subtract the solvent contribution from the diffraction data. The solvent-accessible void volume per unit cell was calculated to be 371 $Å^3$, corresponding to approximately 104 electrons, which is equivalent to 4.33 methanol molecules per average unit cell. The formula of the compound was adjusted to include the estimated solvent content, and all dependent crystallographic parameters were recalculated accordingly.

Powder X-ray Diffraction (PXRD). The X-ray powder patterns were taken with Bruker D8 Discoverer powder diffractometer using Cu Kα radiation at a wavelength of λ = 0.154 18 nm and line detector LYNXEYE XE. Powder samples were loaded on silicon holder (6° off cut from (111)). The measurement was performed in the range of 5–90° 2θ with a step 0.02° 2θ and 1 s/step measurement time.

Differential Scanning Calorimetry (DSC) Analysis was performed on a TA Instruments | Waters Discovery DSC 250. Sample were heated separately from room temperature to 300 °C at 10 °C/min.

Ball Milling. The setup used in this study consisted of a NARVA Brand-Erbisdorf Vibrator containing 220V, 30W, 50 Hz engine, which was equipped with a stainless-steel spherical chamber (27 mm diameter) carrying two stainless-steel balls (8 mm diameter, 4 g each). The surface inclusion was prepared by mixing solid **1•CB[7]** and **TPP-*d*$_{12}$** in defined molar ratios following our previously published procedure.[6] **TPP-*d*$_{12}$** (100 mg, 0.212 mmol) was initially ball-milled alone for 5 minutes. Subsequently, the complex **1•CB[7]** (13.93 mg, 0.03 eq, 6.365 μmol) was added, and the two components were ball-milled together in 5-minute intervals (5 × 5 min), with the mill chamber carefully scratched between intervals. The resulting powder was transferred to a vial, which was evacuated and purged with argon three times before being sealed. The vial was then equilibrated in an oven at 70 °C for 24 hours.

Calculations. Those were carried out on the Owens cluster of the Ohio Supercomputer Center in Columbus, OH (23,392-core Dell Intel Xeon E5-2680 v4 machines), with the semiempirical tight-binding method provided by the GFN2-xTB program.[7,8]

2. Synthesis of 1 and Preparation of Host-Guest Complex 1•CB[7]

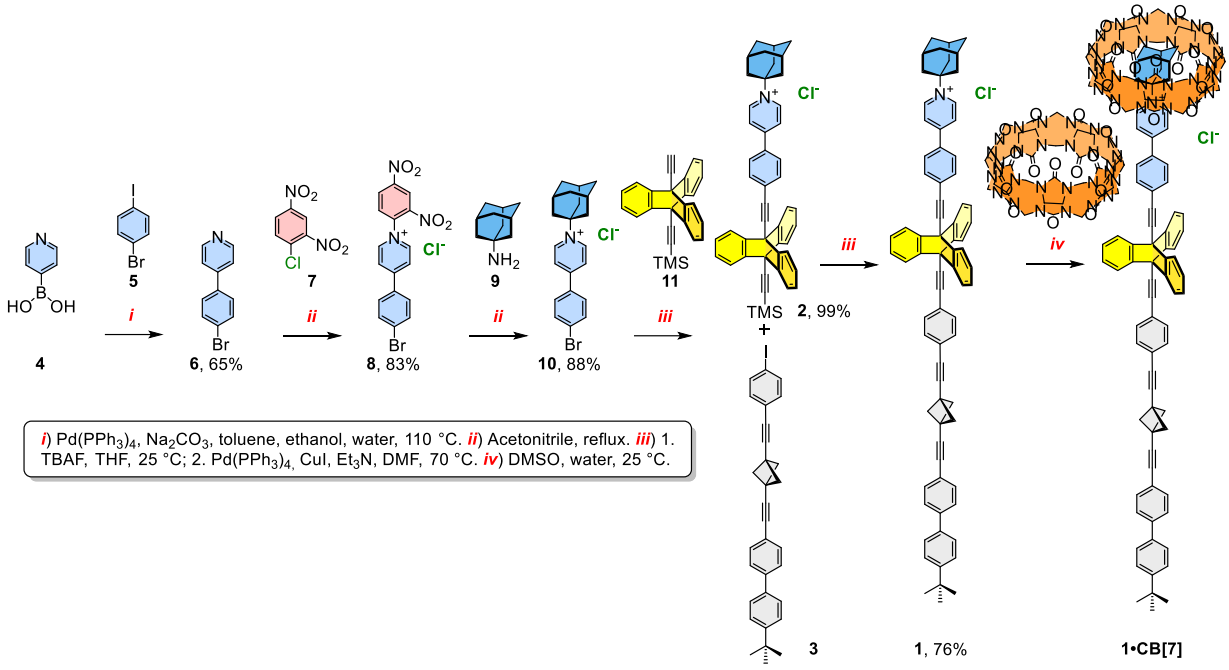

Figure S1. Synthetic strategy to form **1•CB[7]** host-guest complex.

Compounds **3** and **11** were prepared according to previously published procedure.[9]

Compound 1. A Schlenk flask was loaded with silyl derivative **2** (350 mg, 0.501 mmol, 1.0 equiv.), iodide **3** (317 mg, 0.601 mmol, 1.2 equiv.), $Pd(PPh_3)_4$ (23 mg, 0.020 mmol, 4 mol%), and CuI (3 mg, 0.015 mmol, 3 mol%). Following three vacuum/argon cycles, dry and degassed DMF (8 mL) and triethylamine (4 mL) were added via syringe. Subsequently, a solution of TBAF in THF (1 M, 550 µL, 0.550 mmol) was added to the slightly yellowish suspension. It was stirred in an oil bath at 60 °C for 16 hours and the progress was monitored by ESI+ MS. The reaction mixture was cooled to room temperature and diluted with diethyl ether (10 mL). The solids were isolated by centrifugation (3 min, 3000 RPM), then triturated sequentially with diethyl ether (3 × 10 mL), water (3 × 10 mL), methanol (2 × 10 mL), and acetone (3 × 10 mL), with centrifugation (3 min, 3000 RPM) after each step. Finally, the solids were dried under reduced pressure to yield compound **1** as a slightly yellowish powder (392 mg, 0.383 mmol, 76%).

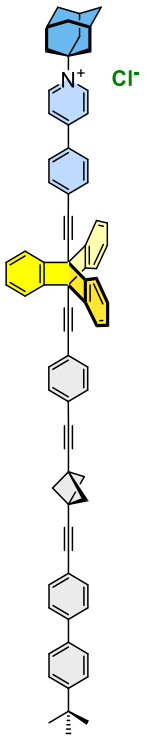

Mp >250 °C (dec.). ^{1}H NMR (500 MHz, DMSO-d_6): δ 1.31 (s, 9H), 1.78 (m, 6H), 2.35 (bs, 9H), 2.55 (s, 6H), 7.23–7.26 (m, 6H), 7.48–7.51 (m, 4H), 7.61-7.63 (m, 4H), 7.66 (d, J = 7.9 Hz, 2H), 7.82–7.86 (m, 6H), 7.94 (d, J = 7.8 Hz, 2H), 8.23 (d, J = 8.0 Hz, 2H), 8.34 (d, J = 8.2 Hz, 2H), 8.61 (d, J = 6.8Hz, 2H), 9.37 (d, J = 6.8 Hz, 2H). ^{13}C {^{1}H} NMR (126 MHz, DMSO-d_6): δ 29.6, 30.3, 30.4, 31.1, 34.4, 34.6, 41.1, 52.4, 58.4, 68.7, 79.8, 80.2, 84.3, 85.7, 88.8, 90.6, 92.4, 92.7, 120.7, 121.7, 122.3, 122.9, 124.5, 125.3, 125.9, 126.35, 126.43, 126.7, 128.8, 132.0, 132.1, 132.5, 133.4, 133.9, 136.3, 140.1, 142.0, 142.8, 143.0, 150.4, 153.4. IR (KBr): 3055, 3033, 2961, 2913, 2874, 2226, 1631, 1604, 1494, 1458, 1452, 1438, 1394, 1362, 1304, 1267, 1201, 1182, 1120, 1102, 1030, 1004, 836, 822, 753, 723, 694, 640, 574, 543, 488 cm^{-1}. MS, *m/z* (%): 988.5 (100%, M^+). HRMS (ESI) *m/z*: $[M]^+$ calcd for $C_{76}H_{62}N^+$ 988.4877; Found 988.4869. Anal. calcd. for $C_{76}H_{62}NCl$: C, 89.08; H, 6.10; N, 1.37. Found: C, 89.42; H, 5.88; N, 1.25.

Supramolecular complex 1•CB[7]. Compound **1** (22.5 mg, 21.4 μmol) was dissolved in DMSO (10 mL) in a round-bottom flask equipped with magnetic stirbar. Solution of cucurbit[7]uril in DMSO (c = 0.7 mmol L^{-1}) was added stepwise to the solution of **1**. The formation of 1:1 complex was followed by ^{1}H NMR of solution aliquots. After addition of 1 equivalent of CB[7] solution (30.6 mL, 21.4 μmol), DMSO was evaporated using Kugelrohr distillation apparatus (110 °C, 1 mbar), yielding supramolecular complex **1•CB[7]** (46.3 mg, 21.2 μmol, 99%) as pale yellow powder.

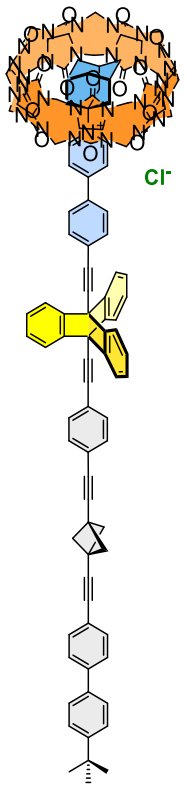

Mp >250 °C (dec.). [*Note: The formation of a Na^+-stabilized trimer of **1•CB[7]** was observed in DMSO-d_6 solution.*[10] *Several peaks corresponding to this compound overlap with those of **1•CB[7]**, making it challenging to precisely assign the hydrogen atoms associated with each species.*] ^{1}H NMR (500 MHz, DMSO-d_6): δ 0.99 (bs, 3H), 1.07–1.15 (m, 1H), 1.23 (br s, 2H), 1.31 (s, 9H), 1.48–1.65 (m, 9H), 2.54 (s, 6H), 4.14–4.47 (m, 14H), 5.37–5.50 (s, 14H), 5.59–5.82 (m, 14H), 7.20–7.30 (m, 6H), 7.44–7.53 (m, 4H), 7.57–7.63 (m, 4H), 7.63–7.69 (m, 2H), 7.80–7.91 (m, 6H), 7.91-7.99 (m, 2H), 8.15–8.25 (m, 2H), 8.33–8.50 (m, 4H), 9.04–9.28 (m, 2H). ^{13}C {^{1}H} NMR (125 MHz, DMSO-d_6): δ 29.1, 30.2, 30.4, 31.1, 33.8, 34.3, 41.2, 51.7, 52.3, 52.4, 58.3, 68.7, 69.9, 79.7, 80.2, 84.4, 85.4, 88.8, 90.4, 92.8, 120.7, 121.6, 122.3, 122.6, 122.9, 124.7, 125.8, 126.3, 126.6, 128.5, 131.9, 132.0, 132.5, 133.3, 134.2, 136.2, 140.0, 142.9, 143.5, 150.4, 151.4, 154.5, 155.1. IR (KBr): 3432, 3136, 3066, 2993, 2915, 2878, 1739, 1634, 1605, 1468, 1419, 1375, 1320, 1298, 1252, 1230, 1188, 1151, 1133, 1029, 987, 967, 823, 803, 756, 100, 691, 672, 639, 595, 572, 543, 485, 457 cm^{-1}. MS, *m/z* (%): 2151.8 (100, M^+). HRMS (ESI+) *m/z*: Calcd for $C_{118}H_{104}N_{29}O_{14}^+$ 2150.8312; Found 2150.8287. Anal. calcd. for $C_{118}H_{104}N_{29}O_{14}Cl$: C, 64.78; H, 4.79; N, 18.57. Found: C, 64.68; H, 5.14; N, 18.48.

Compound 2. A Schlenk flask was loaded with bromide **10** (300 mg, 0.741 mmol, 1.0 equiv.), alkyne **11** (333 mg, 0.889 mmol, 1.2 equiv.), $Pd(PPh_3)_4$ (34 mg, 0.030 mmol, 4 mol%), and CuI (4 mg, 0.022 mmol, 3 mol%). Following three vacuum/argon cycles, dry and degassed DMF (6 mL) and triethylamine (4 mL) were added via syringe. The resulting yellowish reaction mixture was stirred in an oil bath at 60 °C for 16 hours, during which a dense white solid precipitated. The reaction mixture was cooled to room temperature and diluted with diethyl ether (10 mL). The solids were isolated by centrifugation (3 min, 3000 RPM), then triturated sequentially with diethyl ether (3 × 8 mL), water (3 × 8 mL) and acetone (3 × 8 mL), with centrifugation (3 min, 3000 RPM) after each step. Finally, the solids were dried under reduced pressure to yield compound **2** as a slightly yellowish solid (516 mg, 0.739 mmol, 99%).

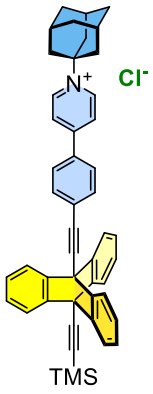

Mp >250 °C (dec.). ^{1}H NMR (400 MHz, DMSO-d_6): δ 0.48 (s, 9H), 1.78 (s, 6H), 2.35 (s, 9H), 7.20–7.27 (m, 6H), 7.70–7.71 (m, 3H), 7.81–7.83 (m, 3H), 8.20–8.22 (m, 2H), 8.32–8.34 (m, 2H), 8.59–8.61 (m, 2H), 9.35–9.36 (m, 2H). ^{13}C {^{1}H} NMR (100 MHz, DMSO-d_6): δ 0.2, 29.5, 34.5, 41.0, 52.3, 52.4, 68.7, 85.7, 92.3, 98.7, 122.0, 122.2, 124.5, 125.2, 126.27, 126.32, 128.7, 133.3, 133.9, 141.9, 142.7, 142.8, 153.4. IR (KBr): 3060, 3032, 2910, 2855, 2180, 1679, 1631, 1603, 1495, 1453, 1446, 1405, 1319, 1306, 1250, 1221, 1128, 1101, 1071, 1040, 1030, 1013, 857, 846, 816, 753, 727, 704, 692, 640, 614, 554, 536, 486 cm^{-1}. MS, *m/z* (%): 662.3 (100%, M^+). HRMS (ESI) *m/z*: $[M]^+$ Calcd for $C_{48}H_{44}SiN^+$ 662.3238; Found 662.3229. Anal. calcd. for $C_{48}H_{44}SiNCl$ (+4H_2O): C, 74.83; H, 6.80; N, 1.82. Found: C, 74.70; H, 6.65; N, 1.68.

4-(4-Bromophenyl)pyridine (6) was prepared according to the published procedure.[11] A

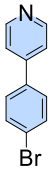

solution of 4-pyridinylboronic acid (**4**) (1.2 g, 10.0 mmol) in ethanol (70 mL) was added to a solution of 1-bromo-4-iodobenzene (**5**) (3.4 g, 12 mmol) in toluene (100 mL), followed by addition of a Na_2CO_3 solution (3.2 g, 30 mmol) in water (30 mL). The mixture was degassed using nitrogen for 10 minutes, after which $Pd(PPh_3)_4$ (580 mg, 0.5 mmol) was added. The resulting crude mixture was vigorously stirred for 2 hours at 110 °C using an oil bath, and then for 18 hours at 100 °C. Finally, the solvent was removed under reduced pressure and the residue was dissolved in CH_2Cl_2 (50 mL) and washed with water (3 × 10 mL). The organic layer was dried over magnesium sulfate, filtered and concentrated under reduced pressure. The crude was submitted to column chromatography on silica (CH_2Cl_2/ethyl acetate = 4/1) yielding **6** as a yellow powder (1.8 g, 7.7 mmol, 77%).

Mp 133.6 – 134.1 °C. ^{1}H NMR ($CDCl_3$, 400 MHz): δ 7.45-7.48 (m, 2H), 7.48-7.52 (m, 2H), 7.59-7.64 (m, 2H), 8.64-8.69 (m, 2H). ^{13}C {^{1}H} NMR ($CDCl_3$, 100 MHz): δ 121.7, 124.1, 128.7, 132.5, 136.8, 148.2, 149.7. IR (KBr): 3074, 3050, 3030, 1905, 1638, 1595, 1568, 1537, 1508, 1475, 1445, 1414, 1393, 1386, 1351, 1324, 1217, 1104, 1078, 1024, 1009, 995, 865, 851, 828,816, 808, 758, 742, 712, 645, 565, 558, 500, 413, 406 cm^{-1}. MS, *m/z* (%): 234.0 (100, $M+H^+$). HRMS (ESI) *m/z*: $[M+H]^+$ Calcd for $C_{11}H_9BrN^+$ 233.9918; Found 233.9915. Anal. calcd. for $C_{11}H_8BrN$: C, 56.44; H, 3.44; N, 5.98. Found: C, 56.51; H, 3.49; N, 5.69.

4-(4-Bromophenyl)-1-(2,4-dinitrophenyl)pyridin-1-ium chloride (8) was prepared

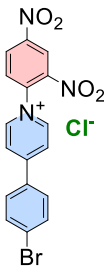

modifying a previously published procedure.[12] A solution of 4-(4-bromophenyl)pyridine (**6**) (7.6 g, 32 mmol) and 1-chloro-2,4-dinitrobenzene (**7**) (22.3 g, 110 mmol) in anhydrous acetonitrile (300 mL) was heated at 75 °C using an oil bath for 2 days under nitrogen. The resulting yellow precipitate was filtered and triturated with hexane (3 × 25 mL) to afford **8** (11.6 g, 27 mmol, 83%) as a light-yellow solid powder.

Mp 198.7 – 200.1 °C. ^{1}H NMR (400 MHz, DMSO-d_6): δ 7.94 (d, J = 8.7 Hz, 2H), 8.22 (d, J = 8.7 Hz, 2H), 8.46 (d, J = 8.7 Hz, 1H), 8.86 (d, J = 7.2 Hz, 2H), 8.90 (dd, J = 8.7 Hz, 1H), 9.14 (d, J = 2.5 Hz, 1H), 9.47 (d, J = 7.2 Hz, 2H).^{13}C {^{1}H} NMR (100 MHz, DMSO-d_6): δ 121.4, 124.1, 127.4, 130.2, 130.7, 132.1, 132.2, 132.9, 138.5, 143.2, 146.1, 149.1, 156.2. IR (KBr): 3106, 3084, 3027, 2977, 2913, 2874, 1636, 1612, 1586, 1541, 1479, 1399, 1339, 1318, 1282, 1250, 1242, 1151, 1127, 1080, 1055, 1006, 913, 889, 836, 742 cm^{-1}. MS, *m/z* (%): 400.0 (100, M^+). HRMS (ESI) *m/z*: $[M]^+$ Calcd for $C_{17}H_{11}BrN_3O_4^+$ 399.9927; Found 399.9947. Anal. calcd. for $C_{17}H_{11}BrClN_3O_4$: C, 46.76; H, 2.54; N, 9.62. Found: C, 46.33; H, 2.39; N, 9.26.

Compound 10. Compound **8** (10.6 g, 24 mmol) and 1-adamantylamine (**9**) (5.5 g, 36 mmol)

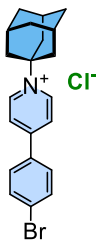

were dissolved in anhydrous acetonitrile (280 mL) under inert atmosphere, yielding a red solution that was stirred for 13 hours at 75 °C. The solvent was then evaporated on rotavapor and the solid residue was triturated with acetone (3 × 25 mL) to afford **10** (8.6 g, 21 mmol, 88%) as an off-white powder.

Mp 240.8 – 241.3 °C. ^{1}H NMR (400 MHz, CD_3CN): δ 1.82–1.84 (m, 6H), 2.32–2.40 (m, 9H), 7.79–7.81 (m, 2H), 7.88–7.90 (m, 2H), 8.29–8.30 (m, 2H), 9.12–9.14 (m, 2H).^{13}C {^{1}H} NMR (100 MHz, CD_3CN): δ 31.1, 35.6, 42.6, 70.4, 125.7, 127.5, 130.9, 133.8, 133.8, 142.6, 155.6. IR (KBr): 3110, 3036, 2909, 2854, 1631, 1587, 1548, 1521; 1484, 1451, 1395, 1360, 1346, 1324, 1308, 1239, 1192, 1145, 1124, 1102, 1074, 1052, 1029, 1005, 985, 974, 833, 815, 778, 739, 652, 568, 498 cm^{-1}. MS, *m/z* (%): 368.1 (100%, M^+). HRMS (ESI) *m/z*: $[M]^+$ Calcd for $C_{21}H_{23}BrN^+$ 368.1008; Found 368.1005. Anal. calcd. for $C_{21}H_{23}NBrCl$ (+2H_2O): C, 57.22; H, 6.17; N, 3.18. Found: C, 57.61; H, 5.86; N, 3.28.

3. Computational Work

Rod **12** and its **CB[7]**-bound analogue were optimized in the gas phase with the semiempirical tight-binding method provided by the GFN2-xTB program[7,8] with a very tight convergence criterion. Conformations were scanned using the same method.

To assess rotation of the adamantyl head group around rod **12** (see Figures 5 and 6 in the narrative), the C(2)(pyridinium)–N(pyridinium)–C(1)(adamantyl)–C(2)(adamantyl) dihedral angle φ was scanned from 0 to 1080°, and an average of the energies obtained from the three full 360° rotations was used. **CB[7]** rotation along the rod **12** axis (see Figures 5 and 7 in the narrative) was assessed by scanning a C(2)(adamantyl)–C(1)(adamantyl)–N(pyridinium)–C(carbonyl, **CB[7]**) dihedral angle ω using the same ranges.

To determine the **CB[7]** tilt angle θ relative to rod **12** (see Figures 5 and 8 in the narrative), energies were scanned by varying the distance between the pyridinium C(4) atom and the nearest oxygen at the **CB[7]** rim. For each optimized assembly along the scan, the tilt angle was calculated with a MATLAB routine using the guest N(pyridinium)-C(adamantyl) vector and a fitted plane across the 14 equatorial carbon atoms of **CB[7]**.

The binding affinity of rod **12** towards **CB[7]** in the gas phase was obtained from the total free energy of the host-guest complex subtracted by the total free energies of the free components. Vibrational analysis to extract the enthalpic and entropic contributions to the free energies was also carried out with the GFN2-xTB program.

4. Assignment of ^{1}H and ^{13}C NMR Signals

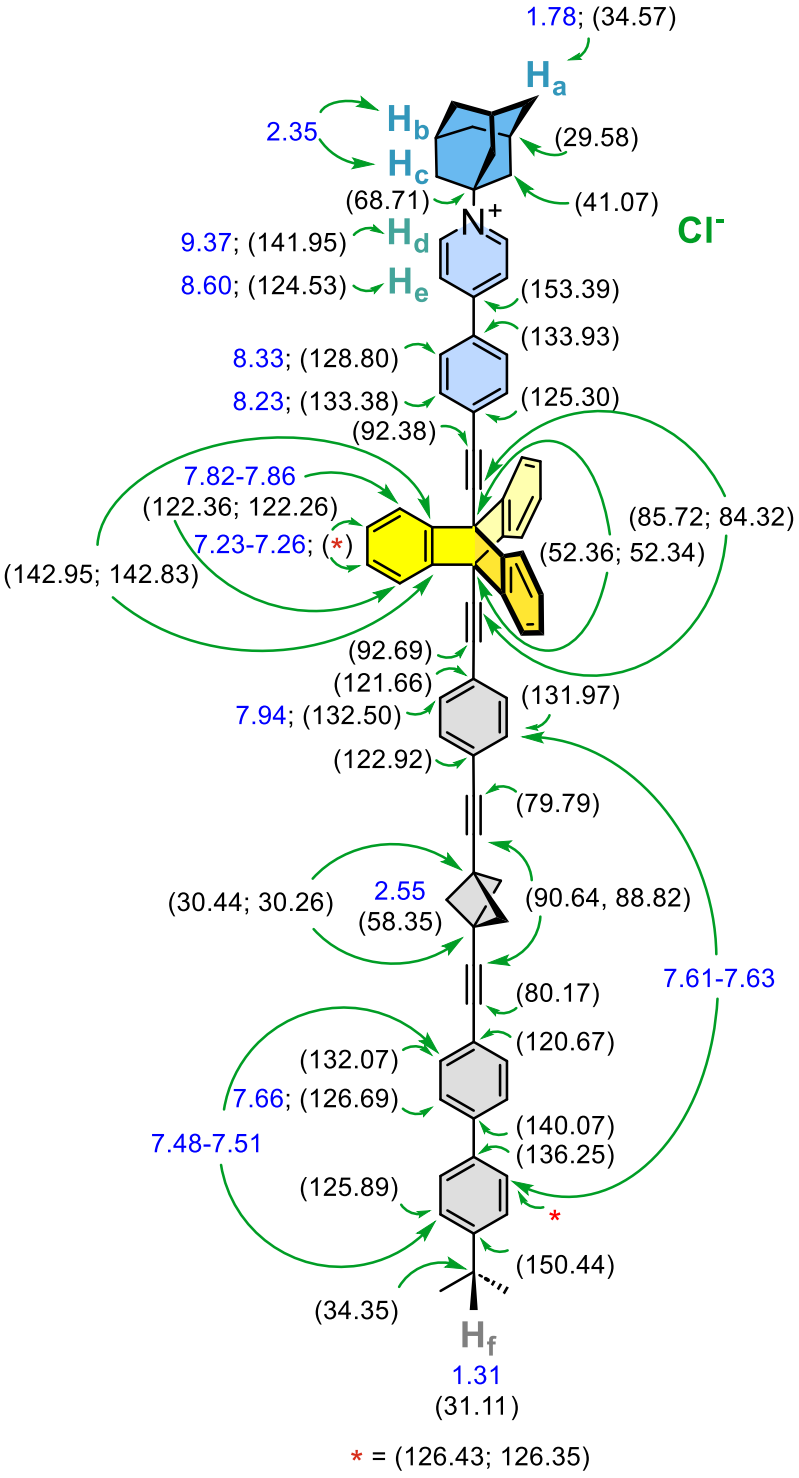

Figure S2. Assignment of ^{1}H (blue) and ^{13}C (black) NMR signals for compound **1** in DMSO-d_6 at 20 °C. Chemical shift values are reported in ppm.

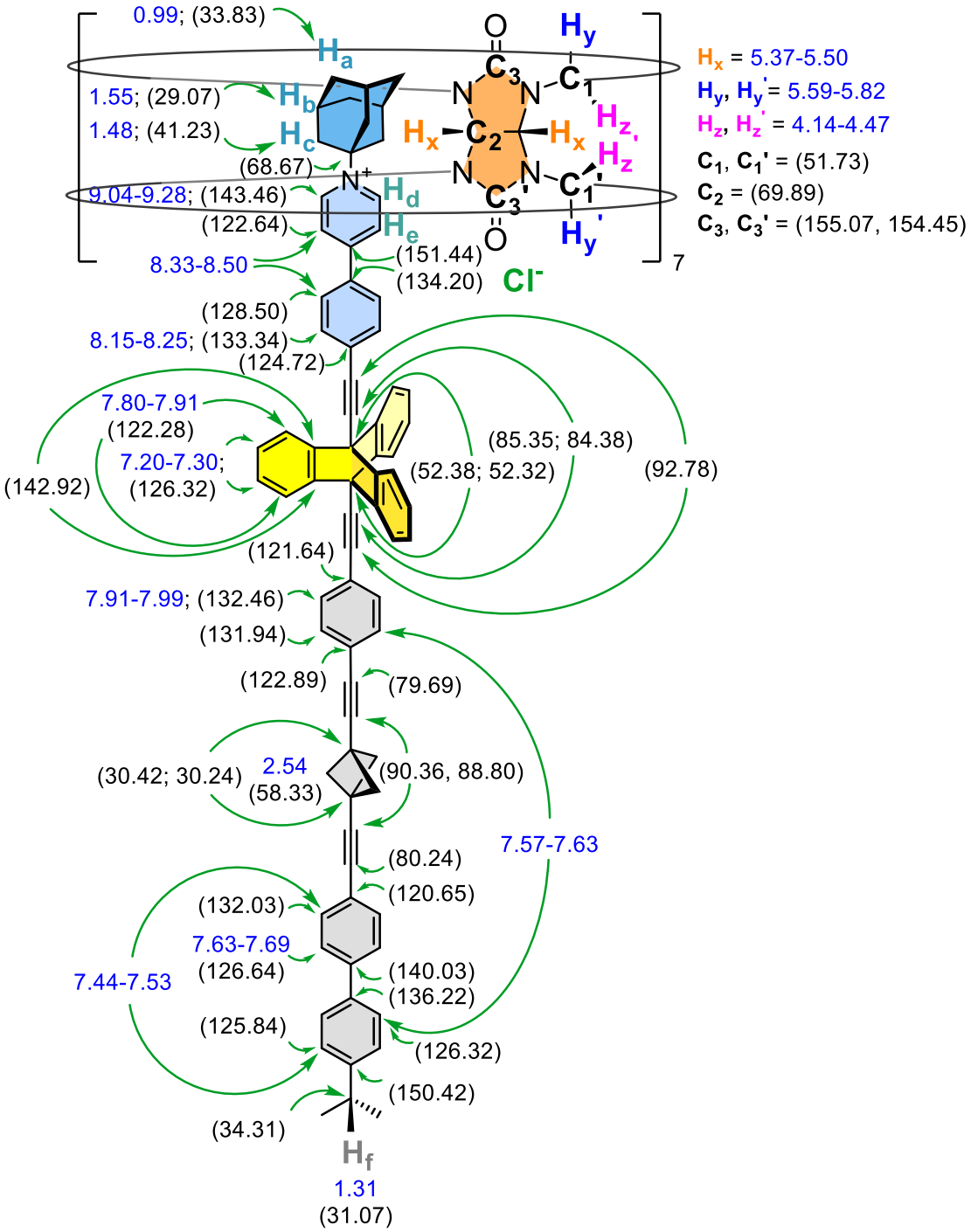

Figure S3. Assignment of ^{1}H (blue) and ^{13}C (black) NMR signals for compound **1•CB[7]** in DMSO-d_6 at 20 °C. Chemical shift values are reported in ppm.

5. Assembly of Supramolecular Complex 1•CB[7] Followed by ^{1}H NMR

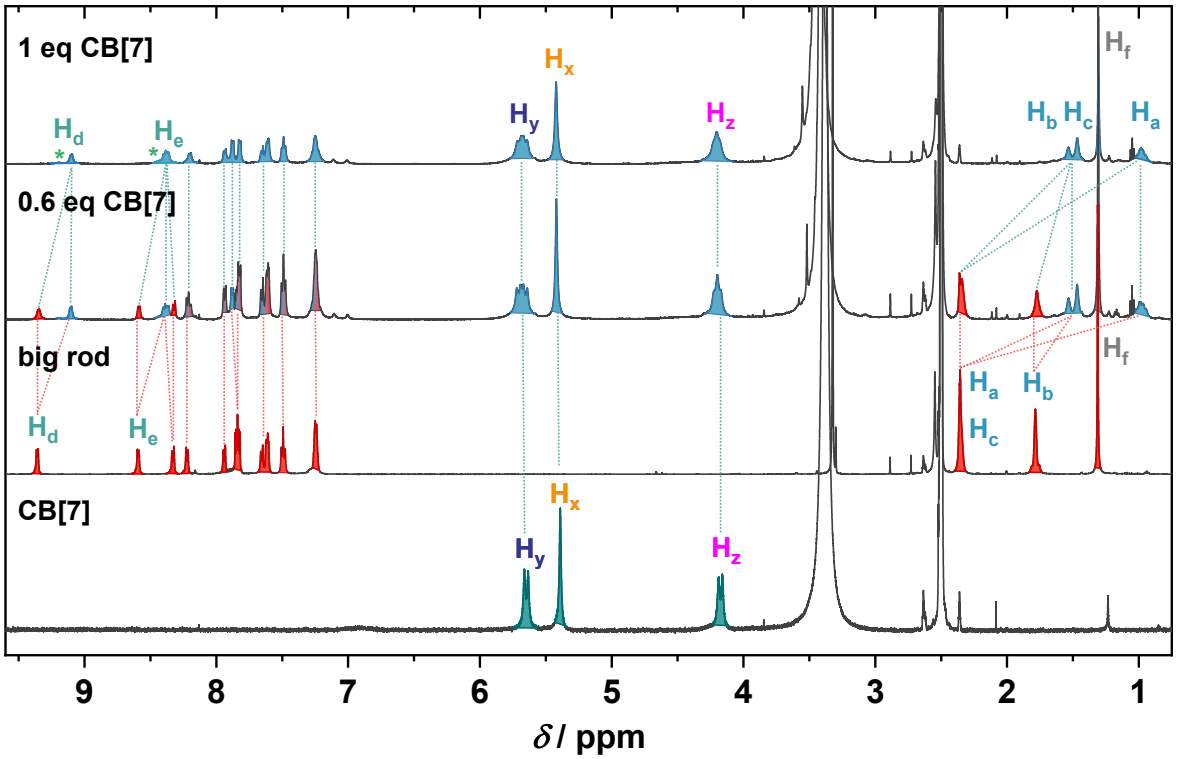

Figure S4. ^{1}H NMR titration of **1** (c = 5 mmol L^{-1}) with CB[7] in DMSO-d_6 at 20 °C. See **Figure S3** for hydrogen atoms labelling.

6. ^{31}P Solid-State NMR of the Surface Inclusion

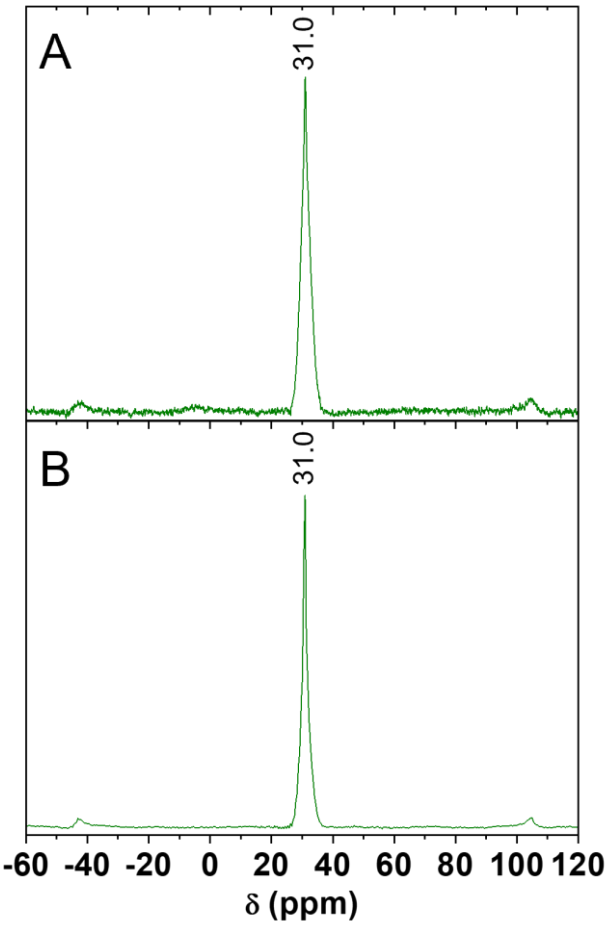

Figure S5. ^{31}P solid-state NMR of **1•CB[7]@TPP-*d*$_{12}$**: single pulse experiment (A) and CP MAS (B).

7. ^{13}C {^{1}H} Solid-State NMR of the Surface Inclusion

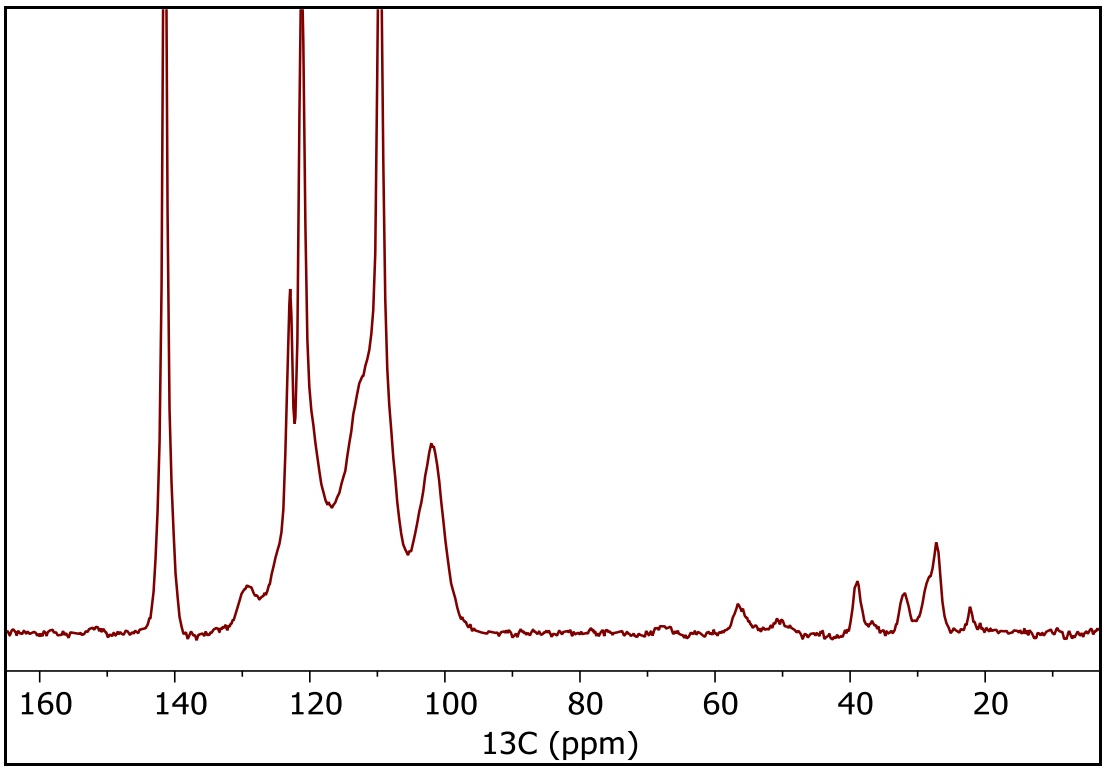

Figure S6. $^{13}C\{^{1}H\}$ NMR spectrum of **1•CB[7]@TPP-*d*$_{12}$** acquired with direct excitation of ^{13}C nuclei (without CP).

8. Differential Scanning Calorimetry

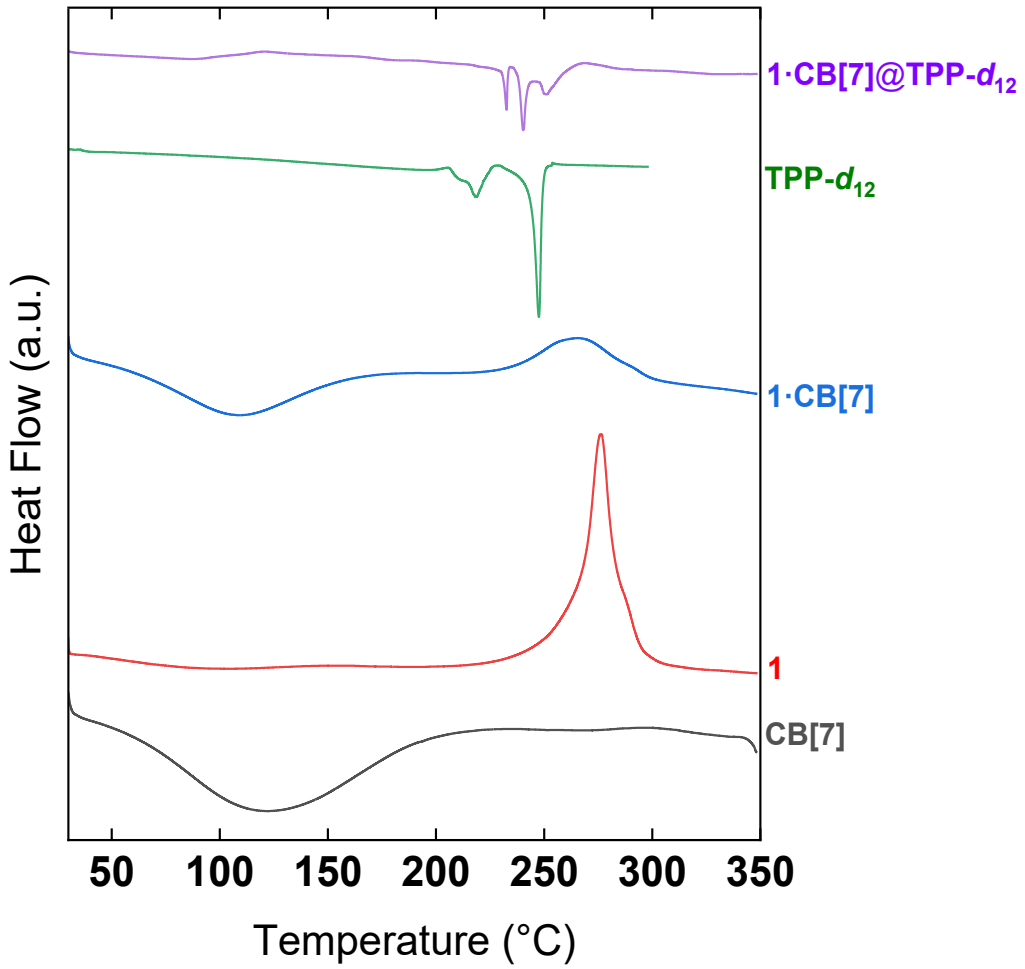

Figure S7. DSC traces of **CB[7]**, compound **1** and their complex, **TPP-d_{12}**, and the supramolecular complex **1•CB[7]@TPP-d_{12}** from +25 to 350 °C scanned at 10°C/min.

9. References

(1) *Modern Supramolecular Chemistry: Strategies for Macrocycle Synthesis*; Diederich, F., Stang, P. J., Tykwinski, R. R., Eds.; WILEY-VCH: Weinheim, 2008.

(2) Sheldrick, G. M. *SHELXT* – Integrated Space-Group and Crystal-Structure Determination. *Acta Crystallogr. Sect. Found. Adv.* **2015**, *71* (1), 3–8. https://doi.org/10.1107/S2053273314026370.

(3) Sheldrick, G. M. Crystal Structure Refinement with *SHELXL*. *Acta Crystallogr. Sect. C Struct. Chem.* **2015**, *71* (1), 3–8. https://doi.org/10.1107/S2053229614024218.

(4) Spek, A. L. Structure Validation in Chemical Crystallography. *Acta Crystallogr. D Biol. Crystallogr.* **2009**, *65* (2), 148–155. https://doi.org/10.1107/S090744490804362X.

(5) Parsons, S.; Flack, H. D.; Wagner, T. Use of Intensity Quotients and Differences in Absolute Structure Refinement. *Acta Crystallogr. Sect. B Struct. Sci. Cryst. Eng. Mater.* **2013**, *69* (3), 249–259. https://doi.org/10.1107/S2052519213010014.

(6) Kaleta, J.; Chen, J.; Bastien, G.; Dračínský, M.; Mašát, M.; Rogers, C. T.; Feringa, B. L.; Michl, J. Surface Inclusion of Unidirectional Molecular Motors in Hexagonal Tris(*o* -Phenylene)Cyclotriphosphazene. *J. Am. Chem. Soc.* **2017**, *139* (30), 10486–10498. https://doi.org/10.1021/jacs.7b05404.

(7) Grimme, S.; Bannwarth, C.; Shushkov, P. A Robust and Accurate Tight-Binding Quantum Chemical Method for Structures, Vibrational Frequencies, and Noncovalent Interactions of Large Molecular Systems Parametrized for All Spd-Block Elements (*Z* = 1–86). *J. Chem. Theory Comput.* **2017**, *13* (5), 1989–2009. https://doi.org/10.1021/acs.jctc.7b00118.

(8) Bannwarth, C.; Ehlert, S.; Grimme, S. GFN2-xTB—An Accurate and Broadly Parametrized Self-Consistent Tight-Binding Quantum Chemical Method with Multipole Electrostatics and Density-Dependent Dispersion Contributions. *J. Chem. Theory Comput.* **2019**, *15* (3), 1652–1671. https://doi.org/10.1021/acs.jctc.8b01176.

(9) Kaleta, J.; Dron, P. I.; Zhao, K.; Shen, Y.; Císařová, I.; Rogers, C. T.; Michl, J. Arrays of Molecular Rotors with Triptycene Stoppers: Surface Inclusion in Hexagonal Tris(*o* -Phenylenedioxy)Cyclotriphosphazene. *J. Org. Chem.* **2015**, *80* (12), 6173–6192. https://doi.org/10.1021/acs.joc.5b00661.

(10) Lončarić, D.; Movahedifar, F.; Štoček, J. R.; Dračínský, M.; Cvačka, J.; Shanshan, G.; Bythell, B.; Císařová, I.; Masson, E.; Kaleta, J. Solvent-Controlled Formation of Alkali and Alkali-Earth-Secured Cucurbituril/Guest Trimers. *Chem. Sci.* **2023**, **14**, 9258-9266. https://doi.org/10.1039/D3SC02032K.

(11) Wang, Y.; Frattarelli, D. L.; Facchetti, A.; Cariati, E.; Tordin, E.; Ugo, R.; Zuccaccia, C.; Macchioni, A.; Wegener, S. L.; Stern, C. L.; Ratner, M. A.; Marks, T. J. Twisted π-Electron System Electrooptic Chromophores. Structural and Electronic Consequences of Relaxing Twist-Inducing Nonbonded Repulsions. *J. Phys. Chem. C* **2008**, *112* (21), 8005–8015. https://doi.org/10.1021/jp8003135.

(12) Yu, H.-J.; Zhou, Q.; Dai, X.; Shen, F.-F.; Zhang, Y.-M.; Xu, X.; Liu, Y. Photooxidation-Driven Purely Organic Room-Temperature Phosphorescent Lysosome-Targeted Imaging. *J. Am. Chem. Soc.* **2021**, *143* (34), 13887–13894. https://doi.org/10.1021/jacs.1c06741.

10. NMR Spectra of Prepared Compounds

^{1}H NMR (500 MHz, DMSO-d_6): Compound **1**

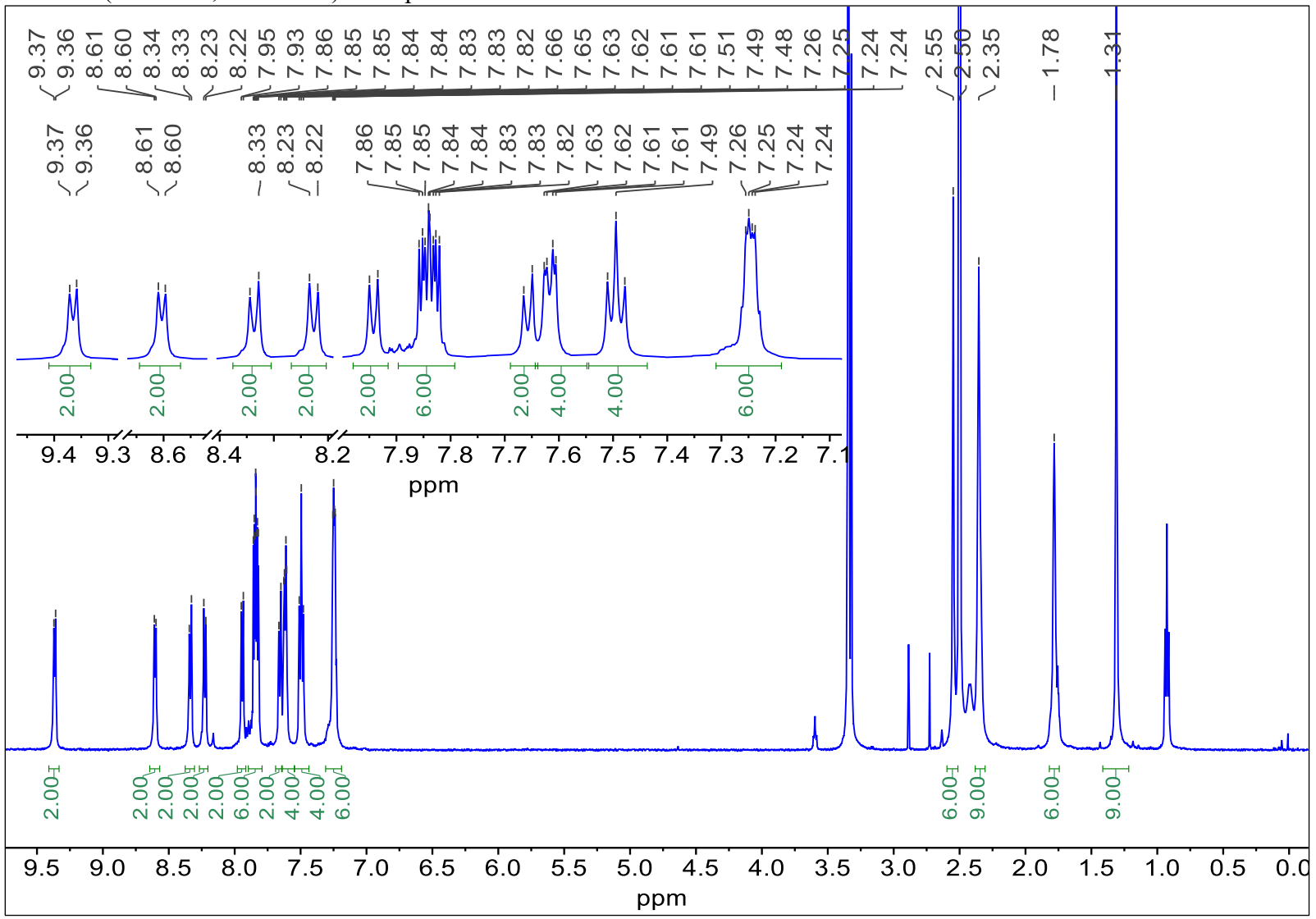

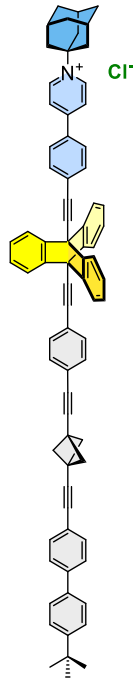

^{13}C {^{1}H} APT NMR (125 MHz, DMSO-d_6): Compound **1**

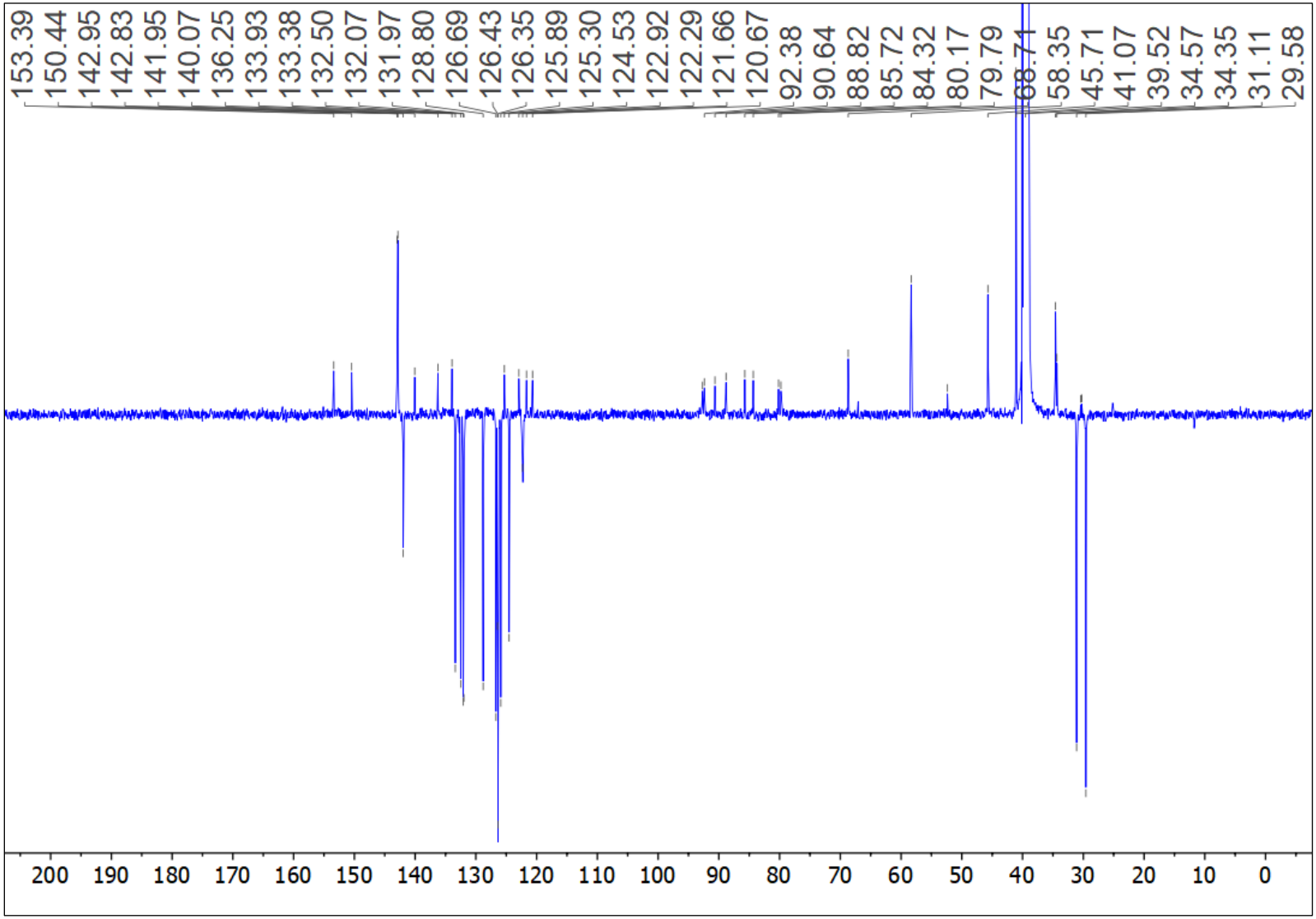

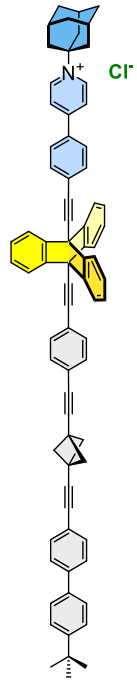

^{1}H - ^{1}H COSY NMR (DMSO-d_6): Compound **1**

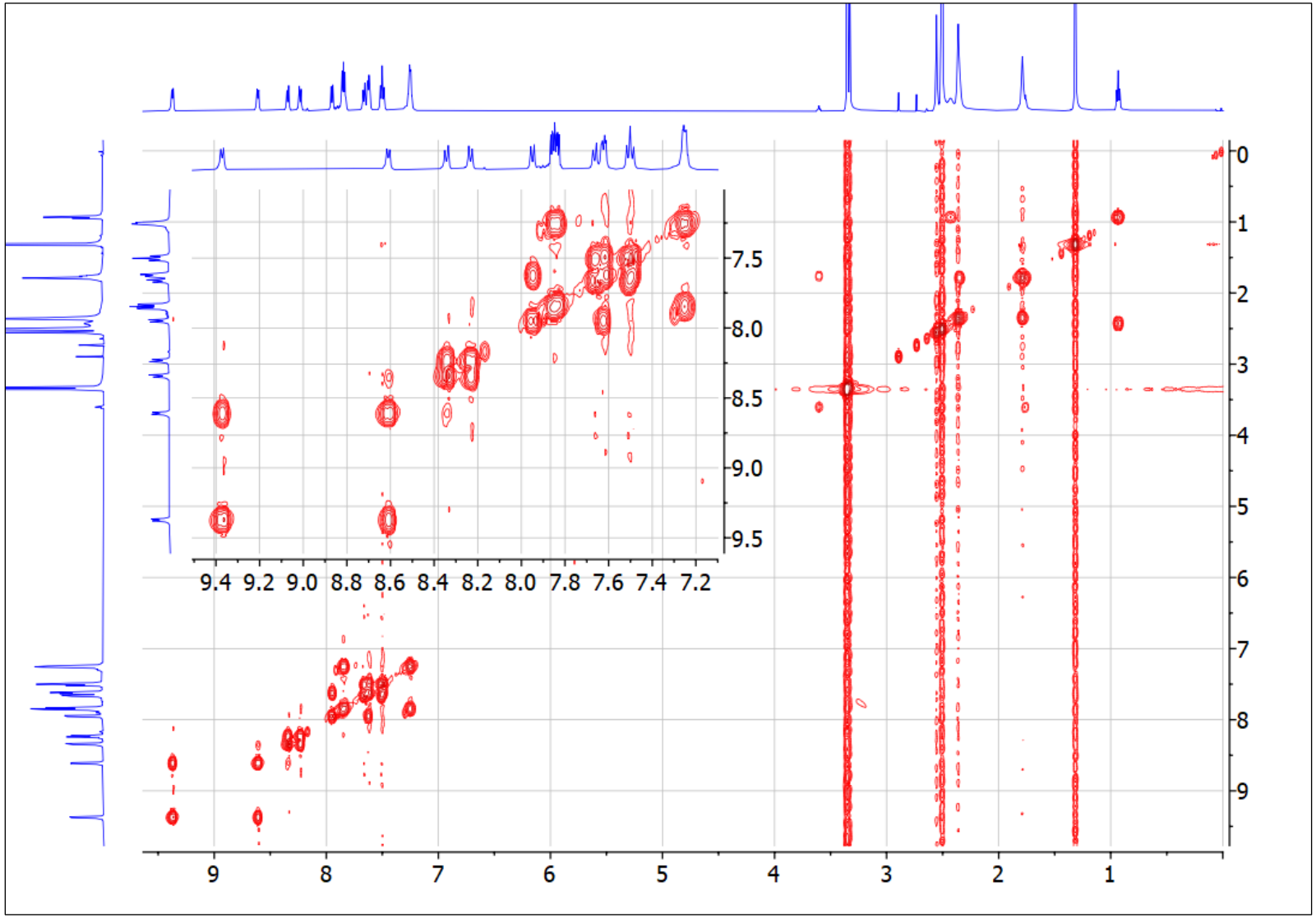

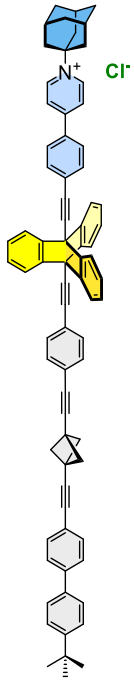

^{1}H - ^{13}C HSQC NMR (DMSO-d_6): Compound **1**

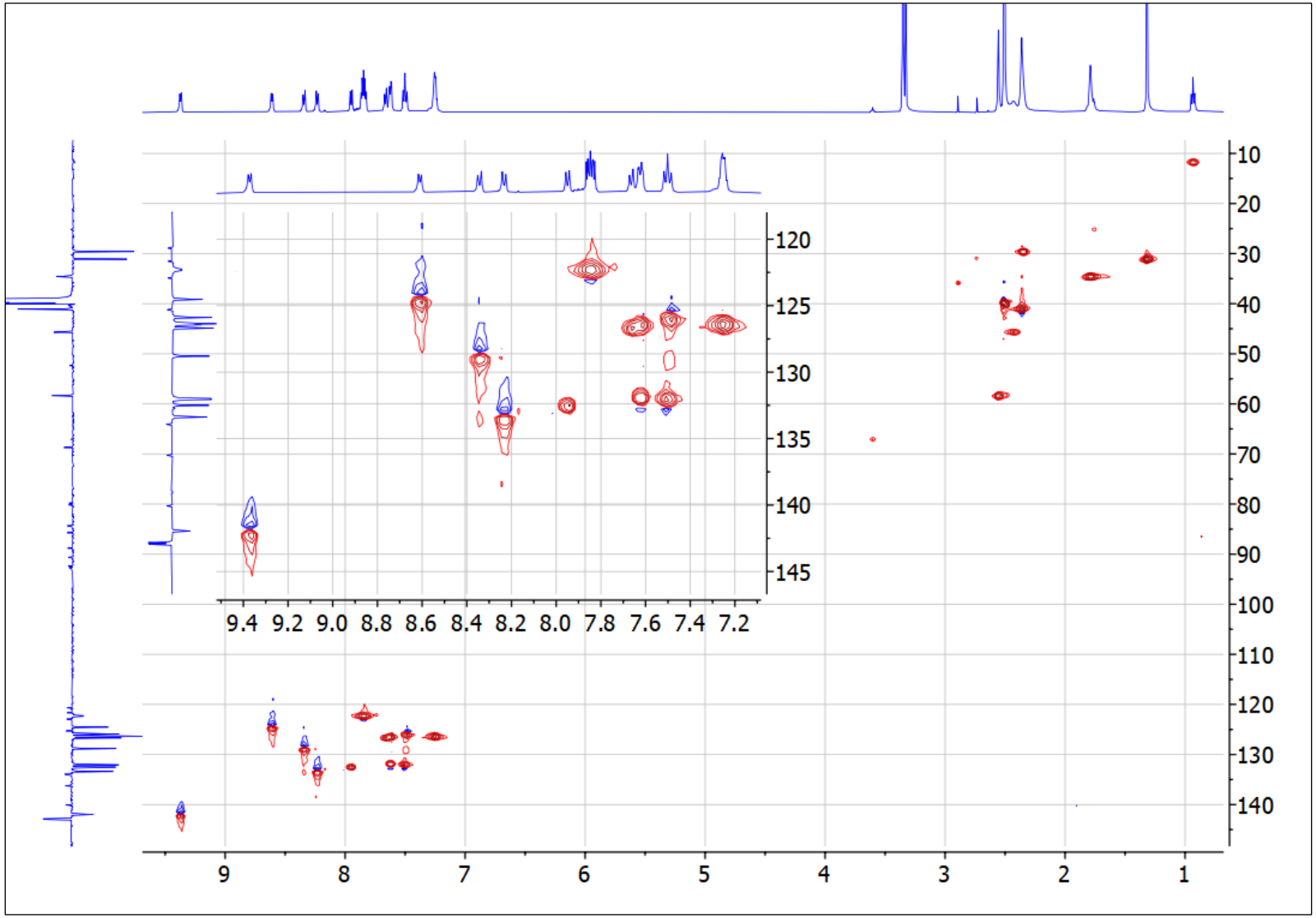

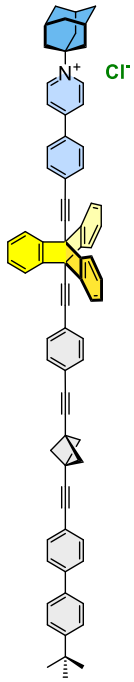

^{1}H - ^{13}C HMBC NMR (DMSO-d_6): Compound **1**

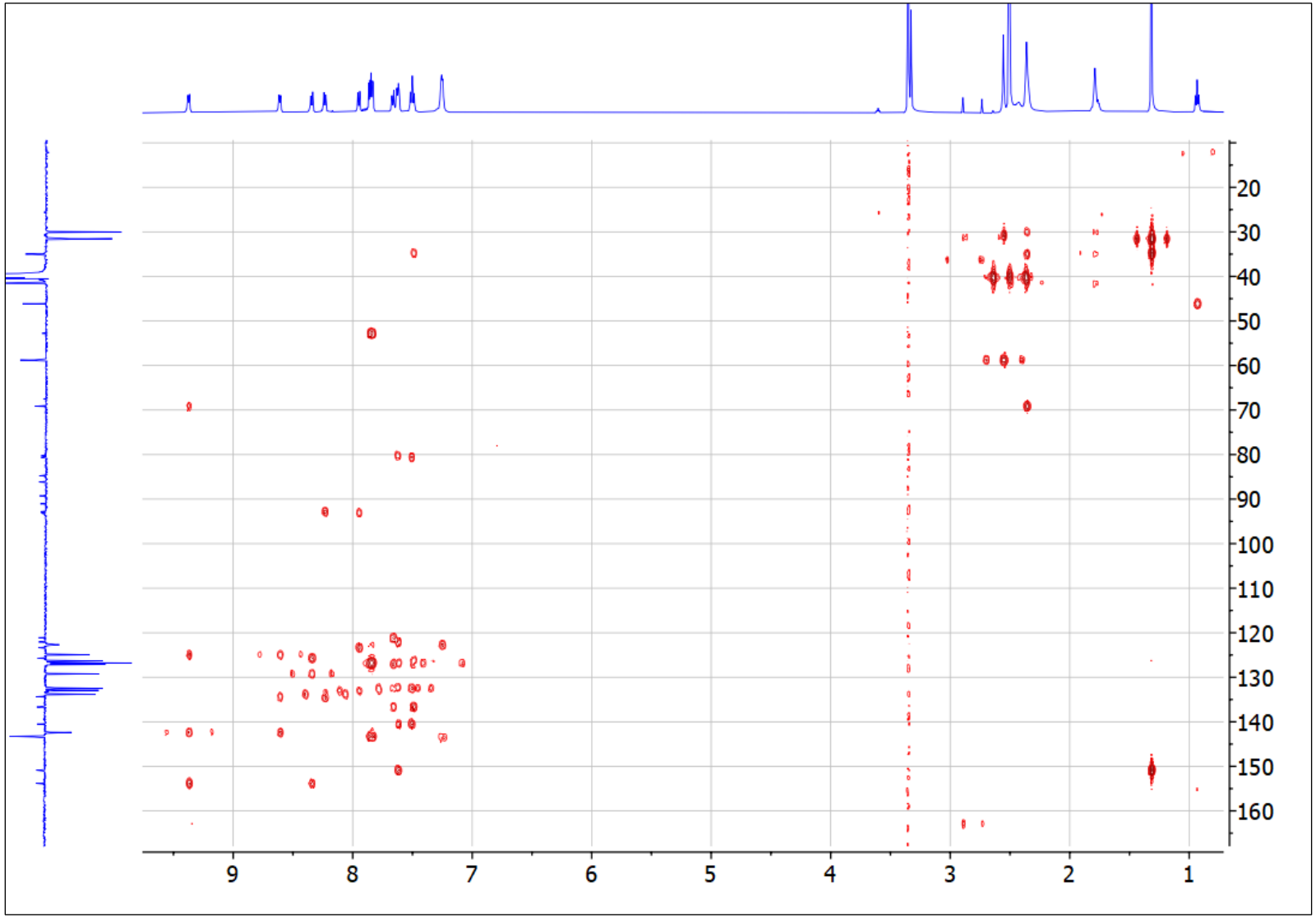

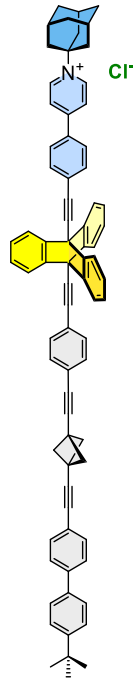

^{1}H NMR (500 MHz, DMSO-d_6): Supramolecular complex **1•CB[7]**. **Asterisks mark peaks of Na^{+}-secured **1•CB[7]** trimer.*

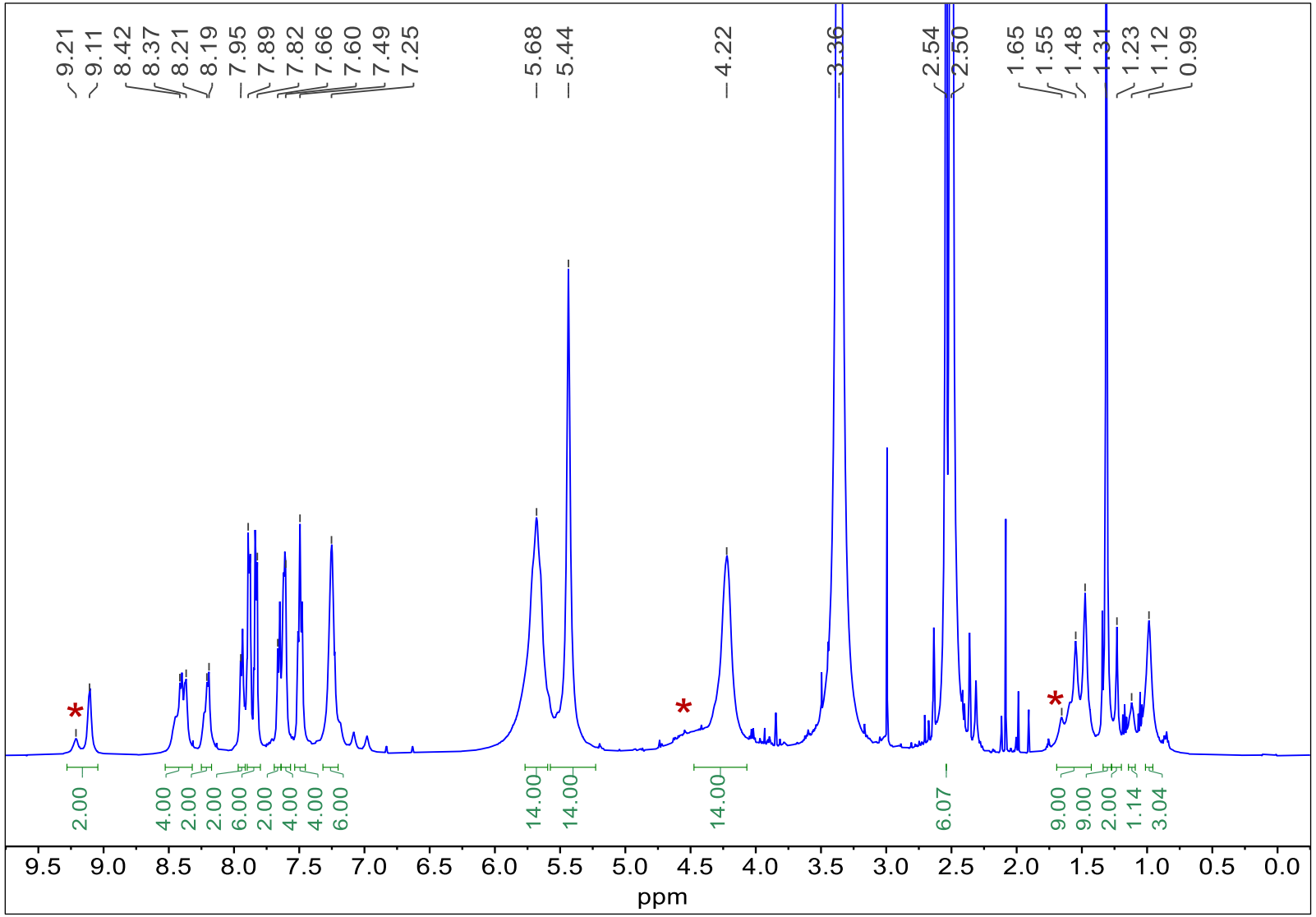

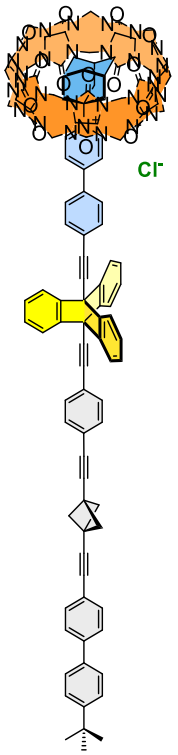

^{13}C {^{1}H} NMR (125 MHz, DMSO-d_6): Supramolecular complex **1•CB[7]**

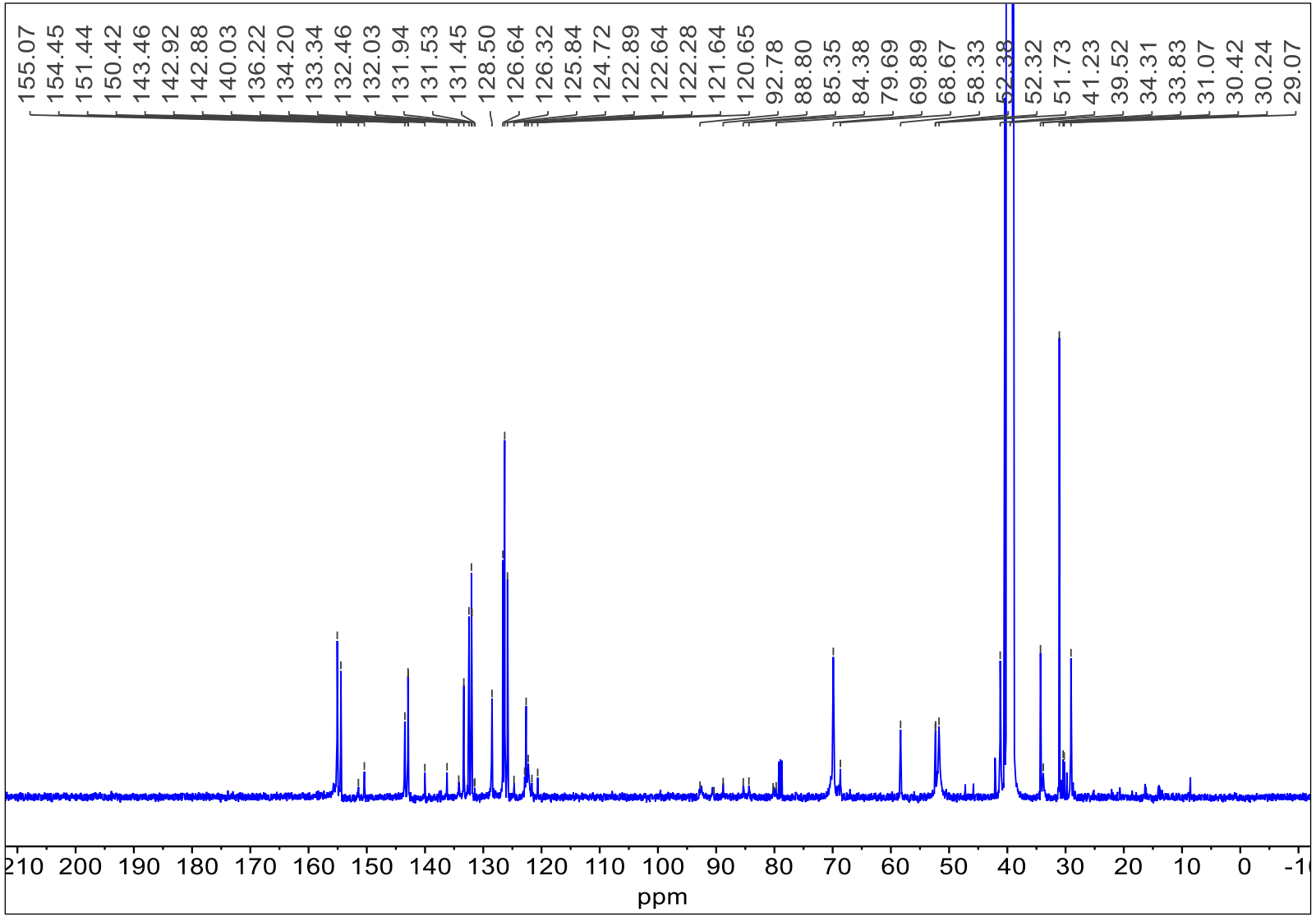

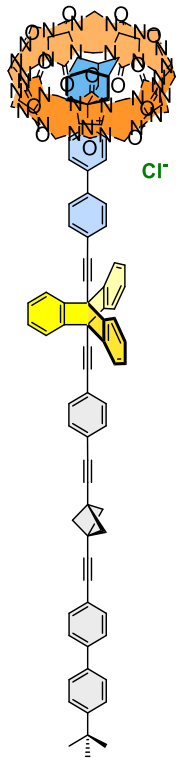

^{13}C {^{1}H} APT NMR (125 MHz, DMSO-d_6): Supramolecular complex **1•CB[7]**

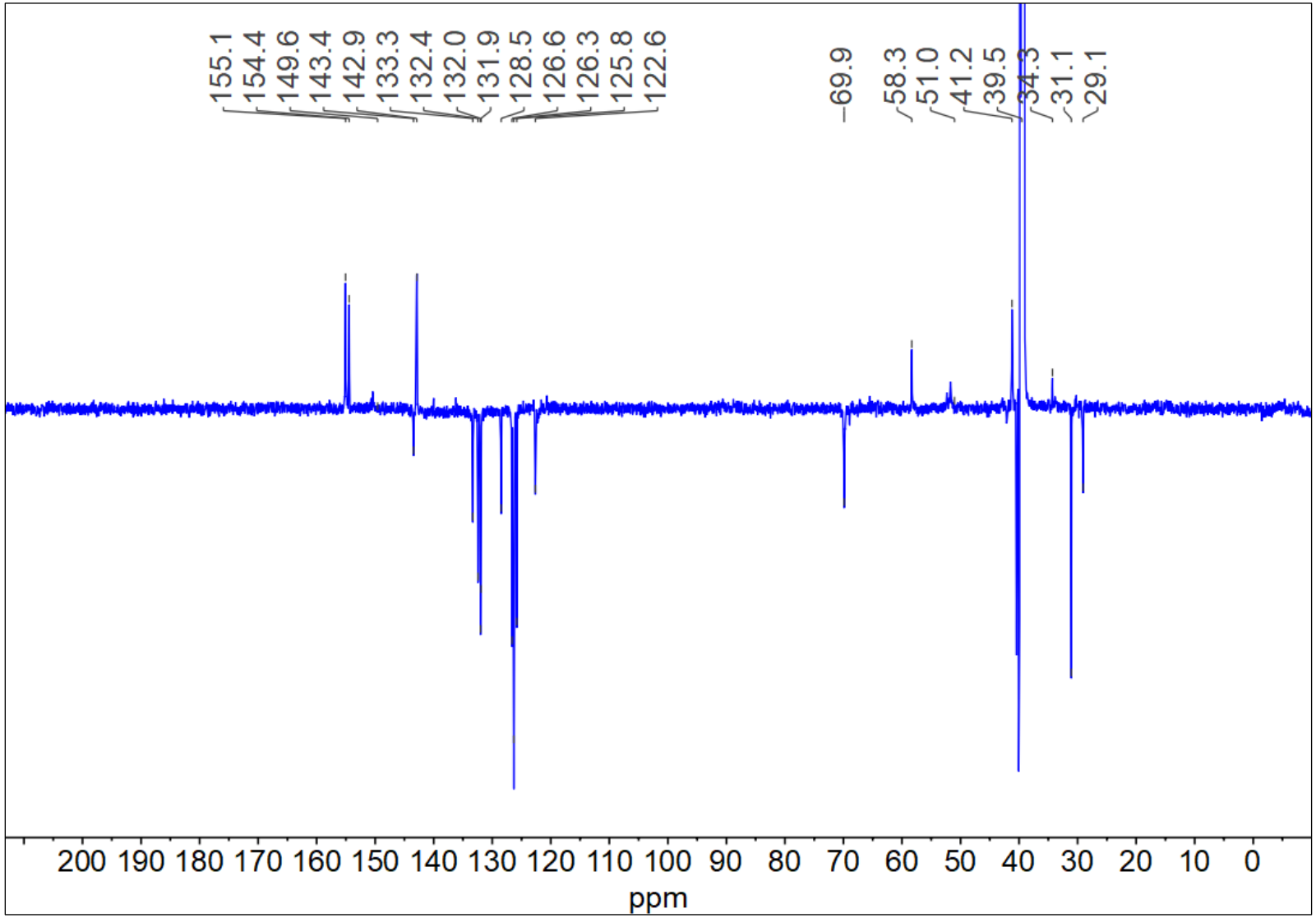

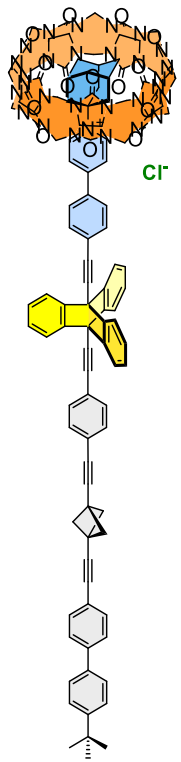

^{1}H – ^{1}H COSY (DMSO-d_6): Supramolecular complex **1•CB[7]**

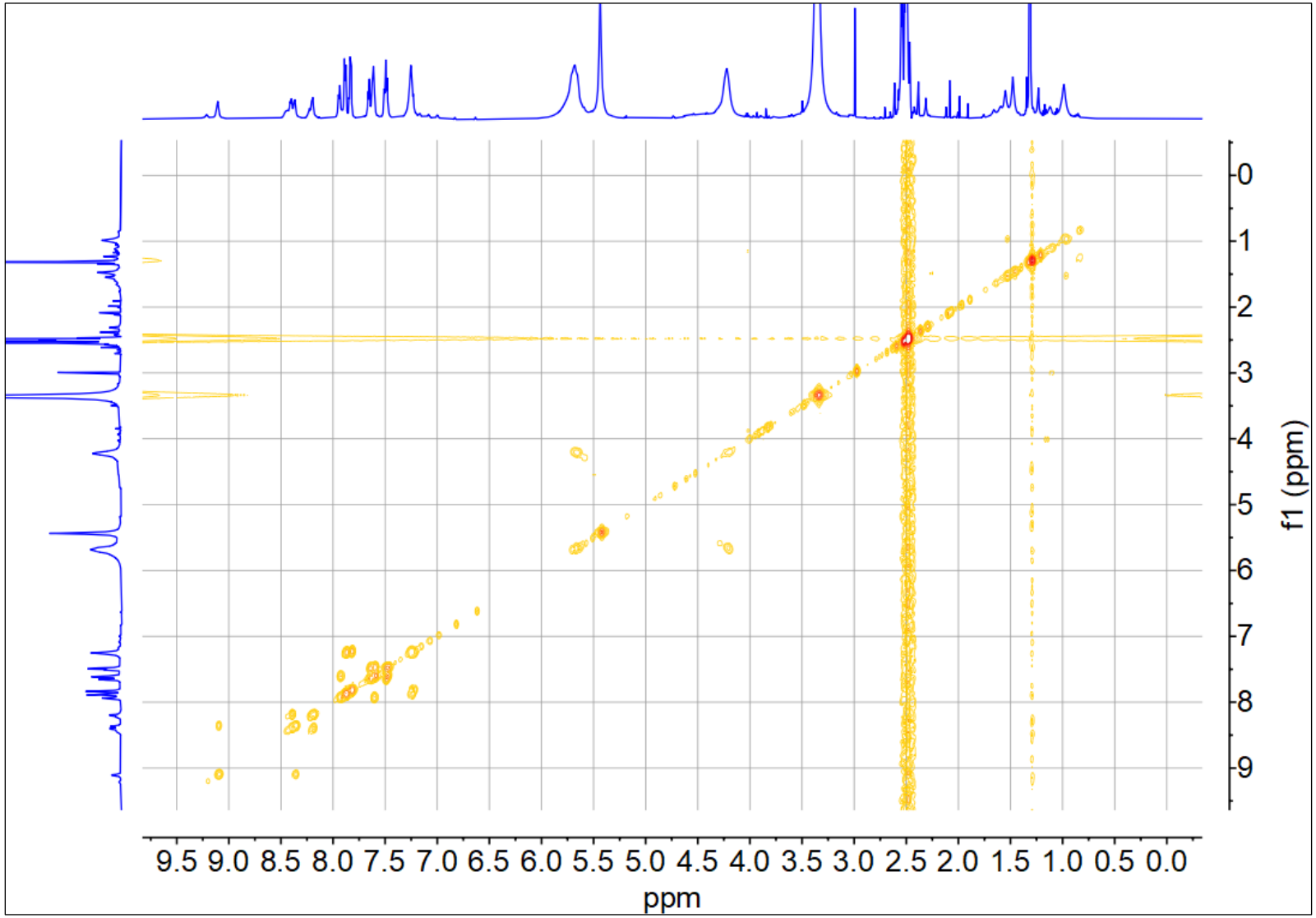

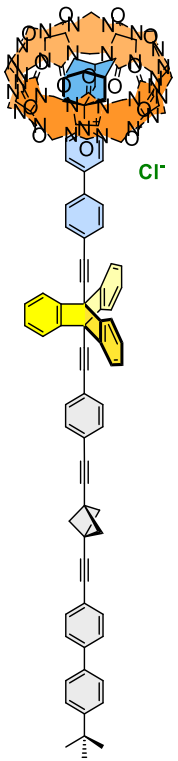

^{1}H – ^{13}C HSQC (DMSO-d_6): Supramolecular complex **1•CB[7]**

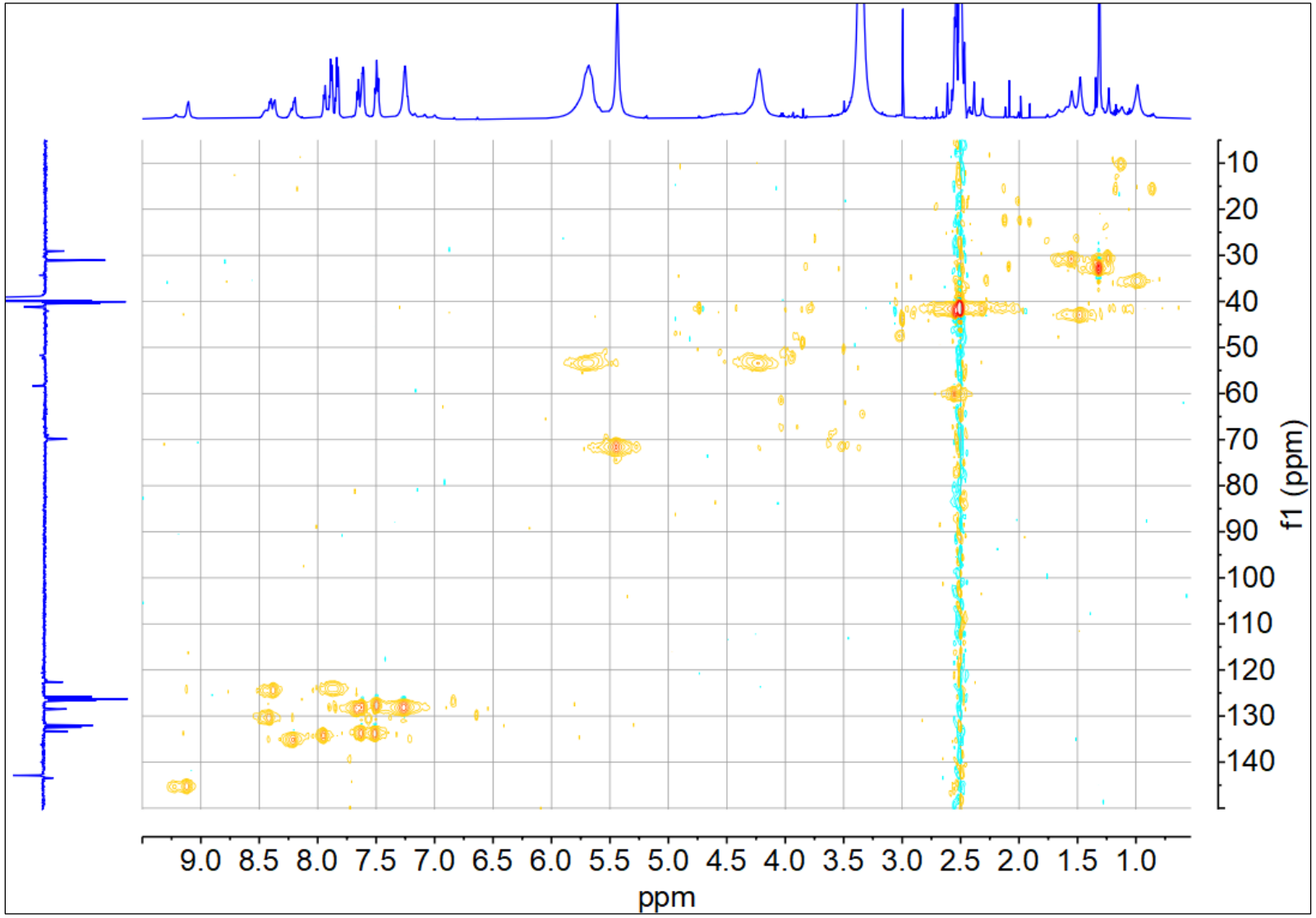

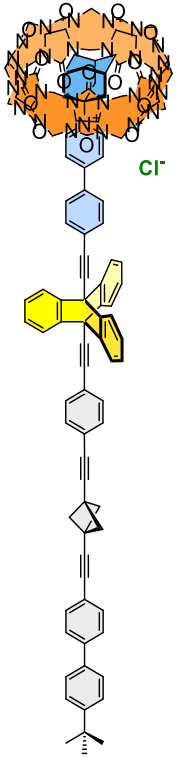

^{1}H – ^{13}C HMBC (DMSO-d_6): Supramolecular complex **1•CB[7]**

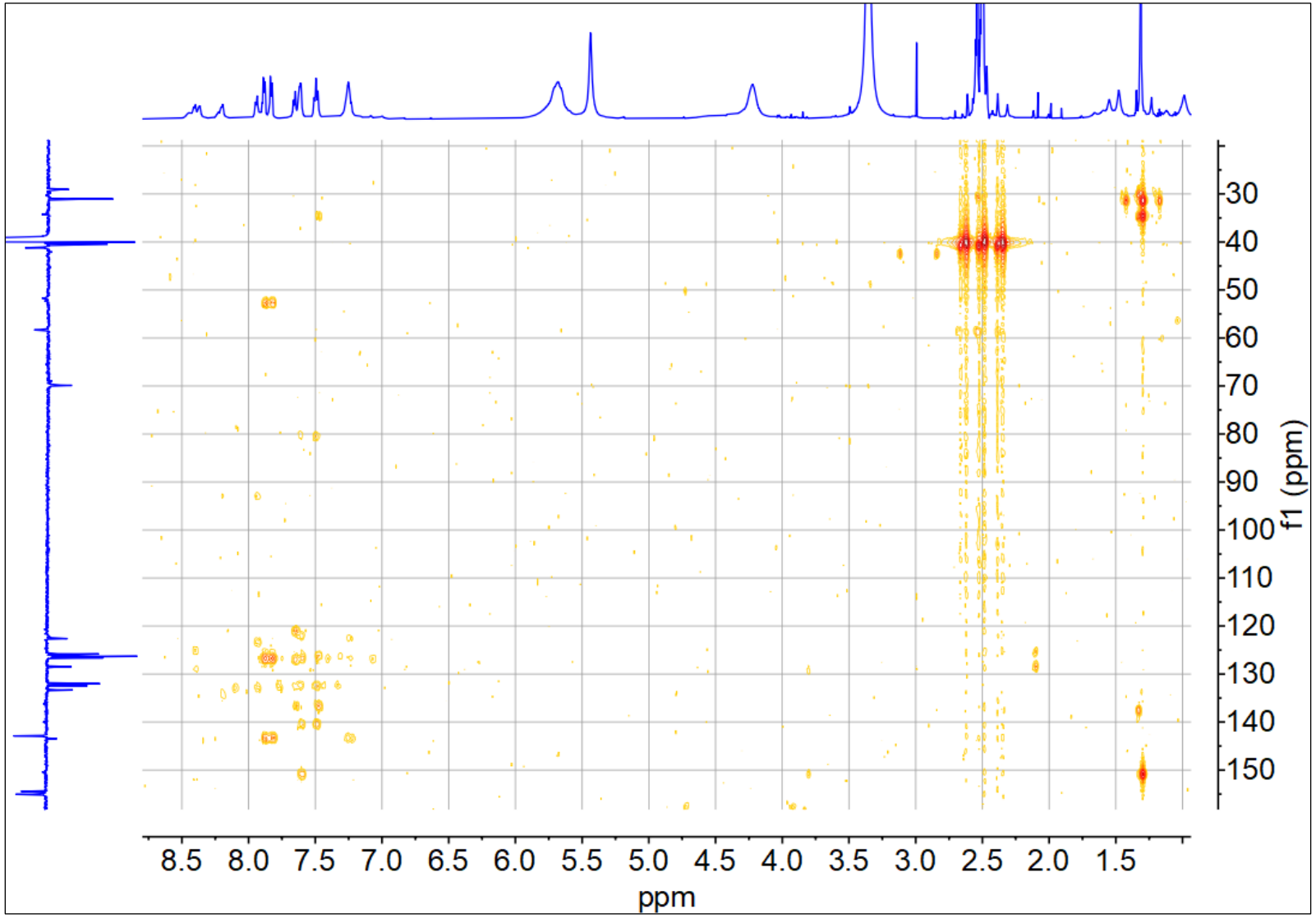

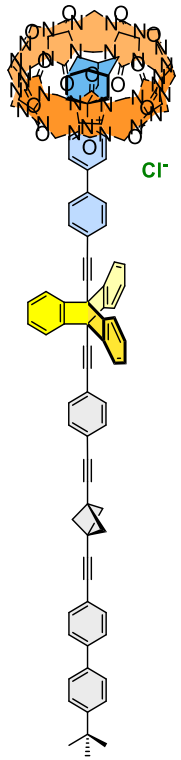

^{1}H NMR (500 MHz, DMSO-d_6): Compound **2**

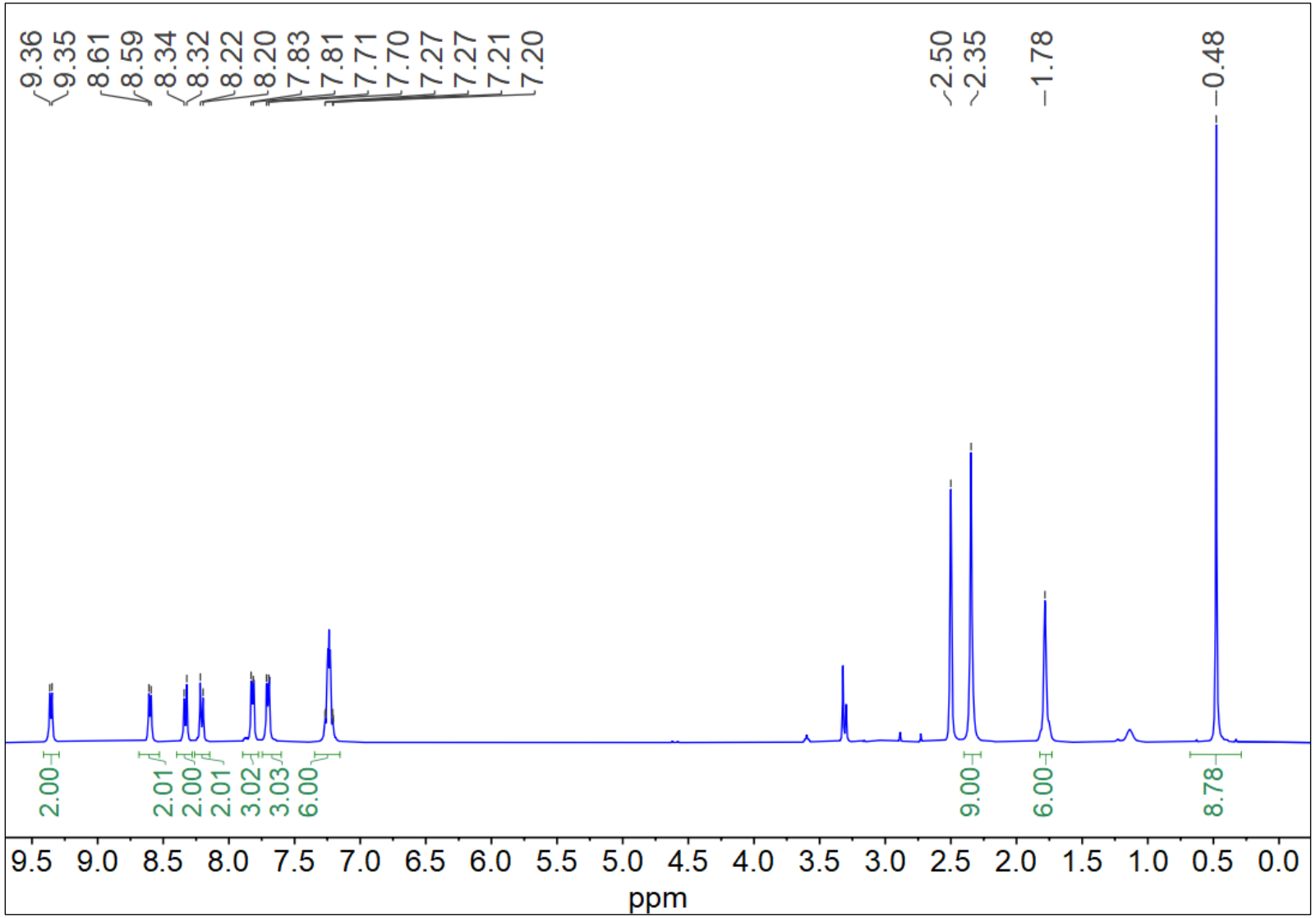

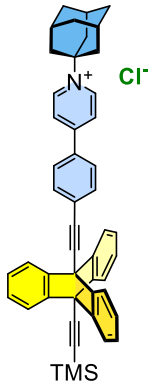

^{13}C {^{1}H} NMR (100 MHz, DMSO-d_6): Compound **2**

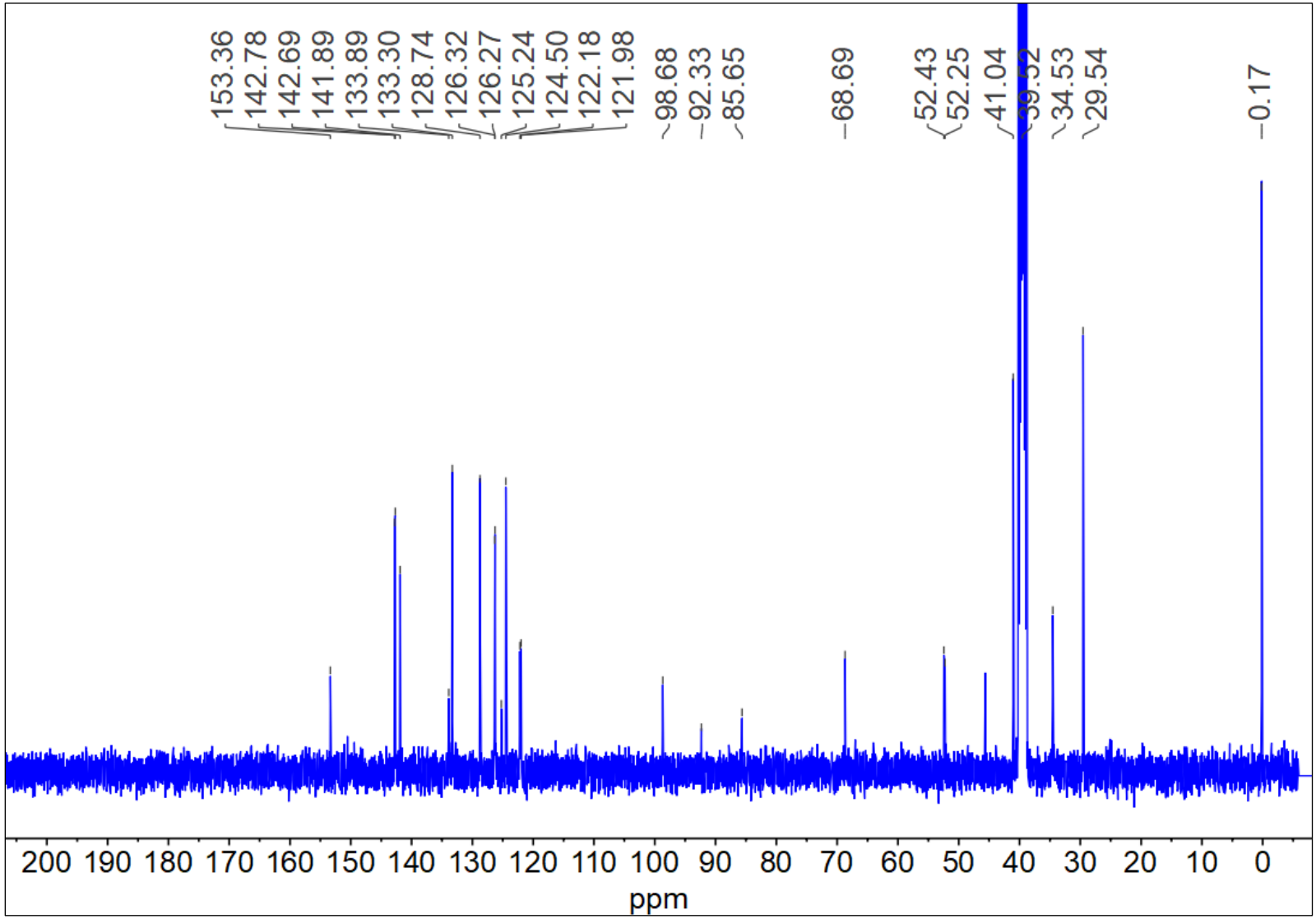

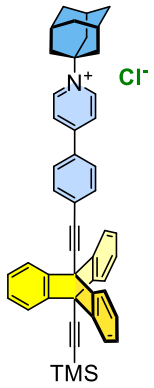

^{13}C APT NMR (100 MHz, DMSO-d_6): Compound **2**

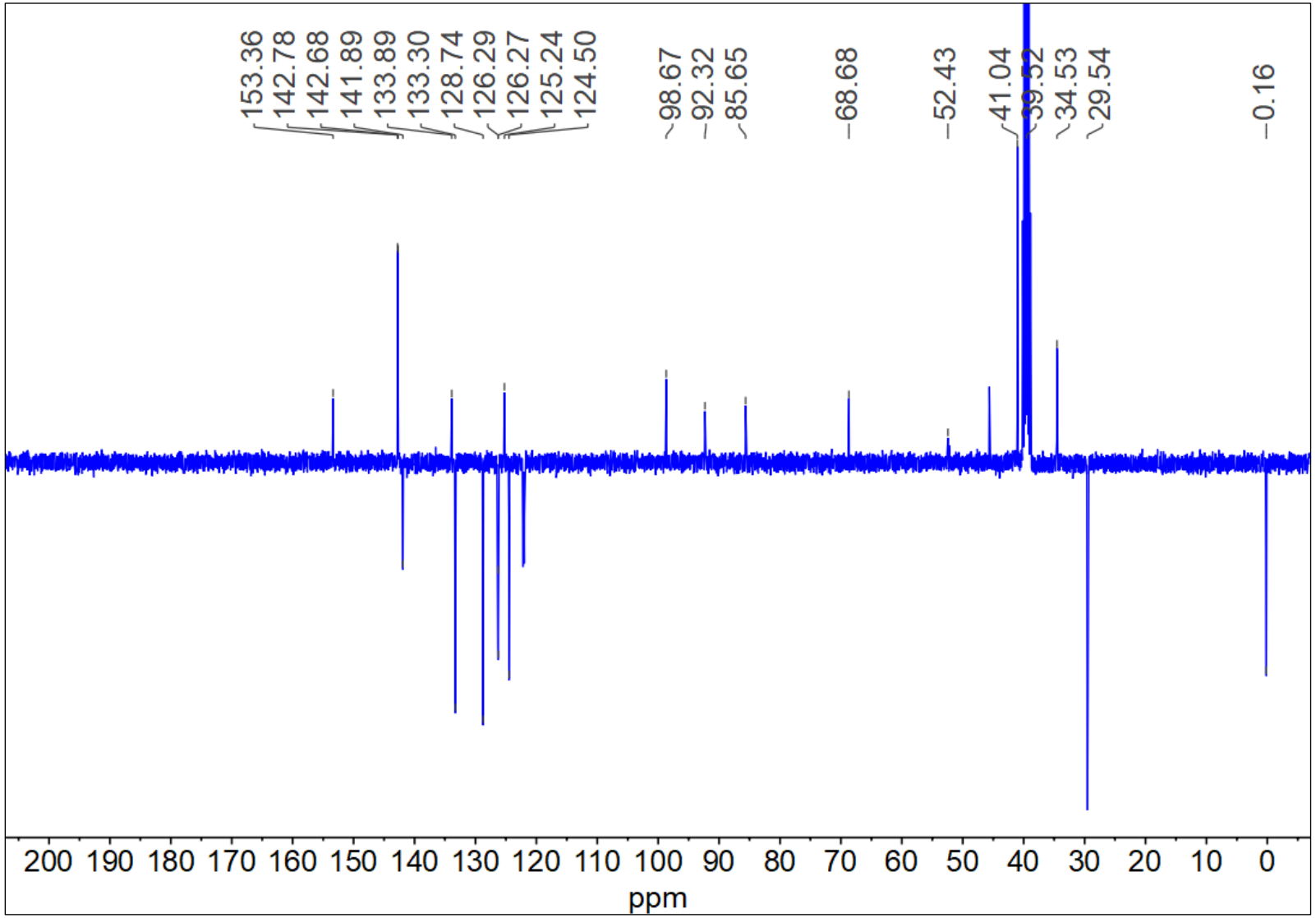

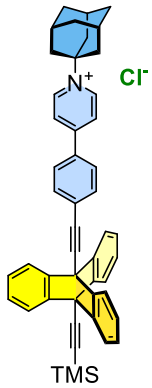

^{1}H – ^{1}H COSY (DMSO-d_6): Compound **2**

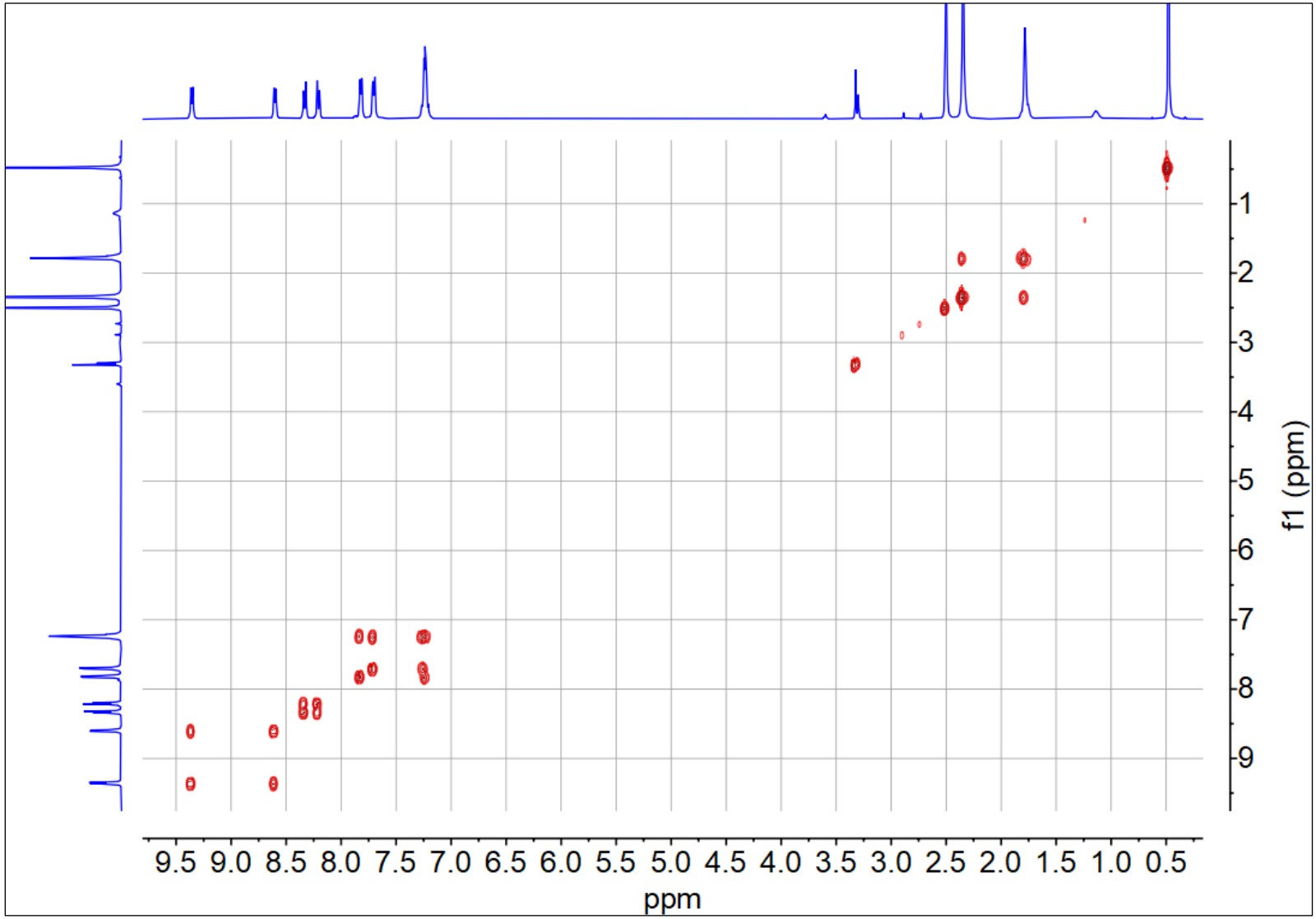

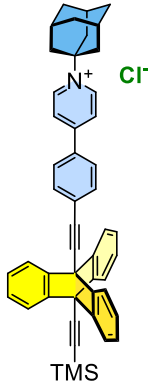

^{1}H – ^{13}C HSQC (DMSO-d_6): Compound **2**

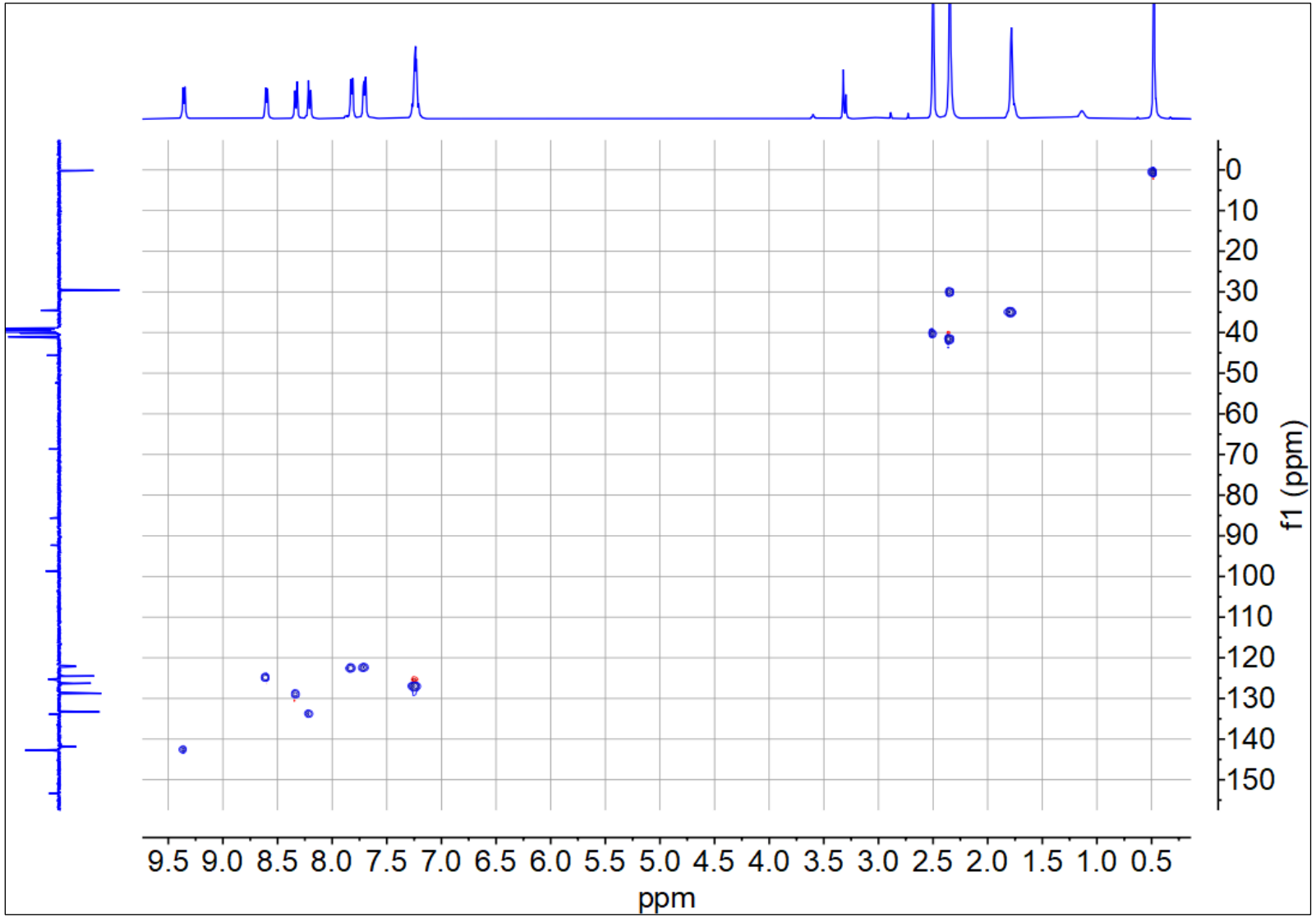

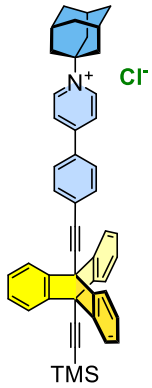

^{1}H – ^{13}C HMBC (DMSO-d_6): Compound **2**

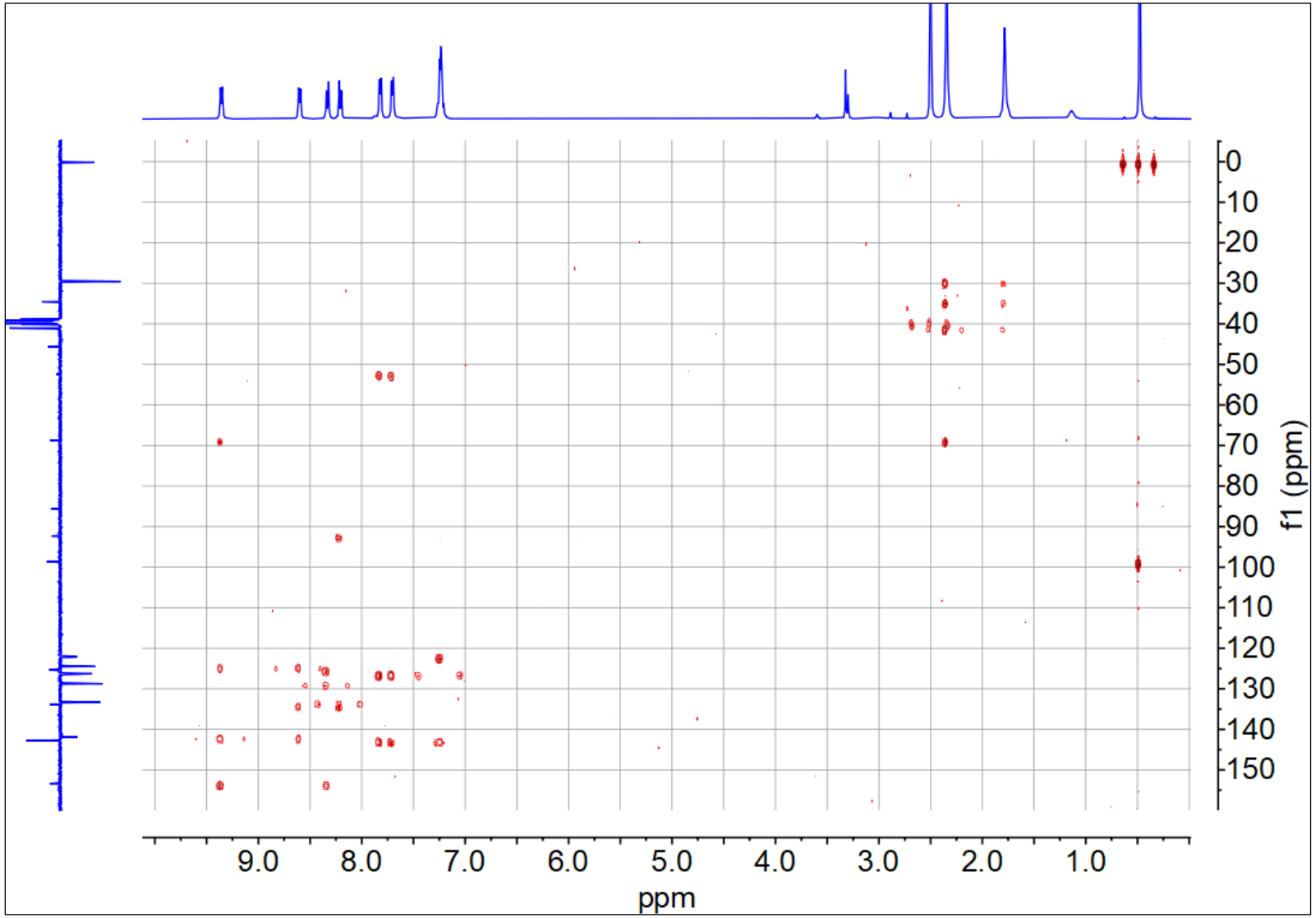

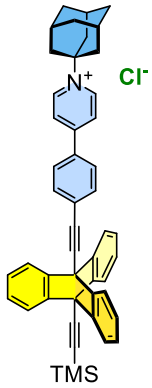

^{1}H NMR (400 MHz, $CDCl_3$): 4-(4-Bromophenyl) pyridine (**6**)

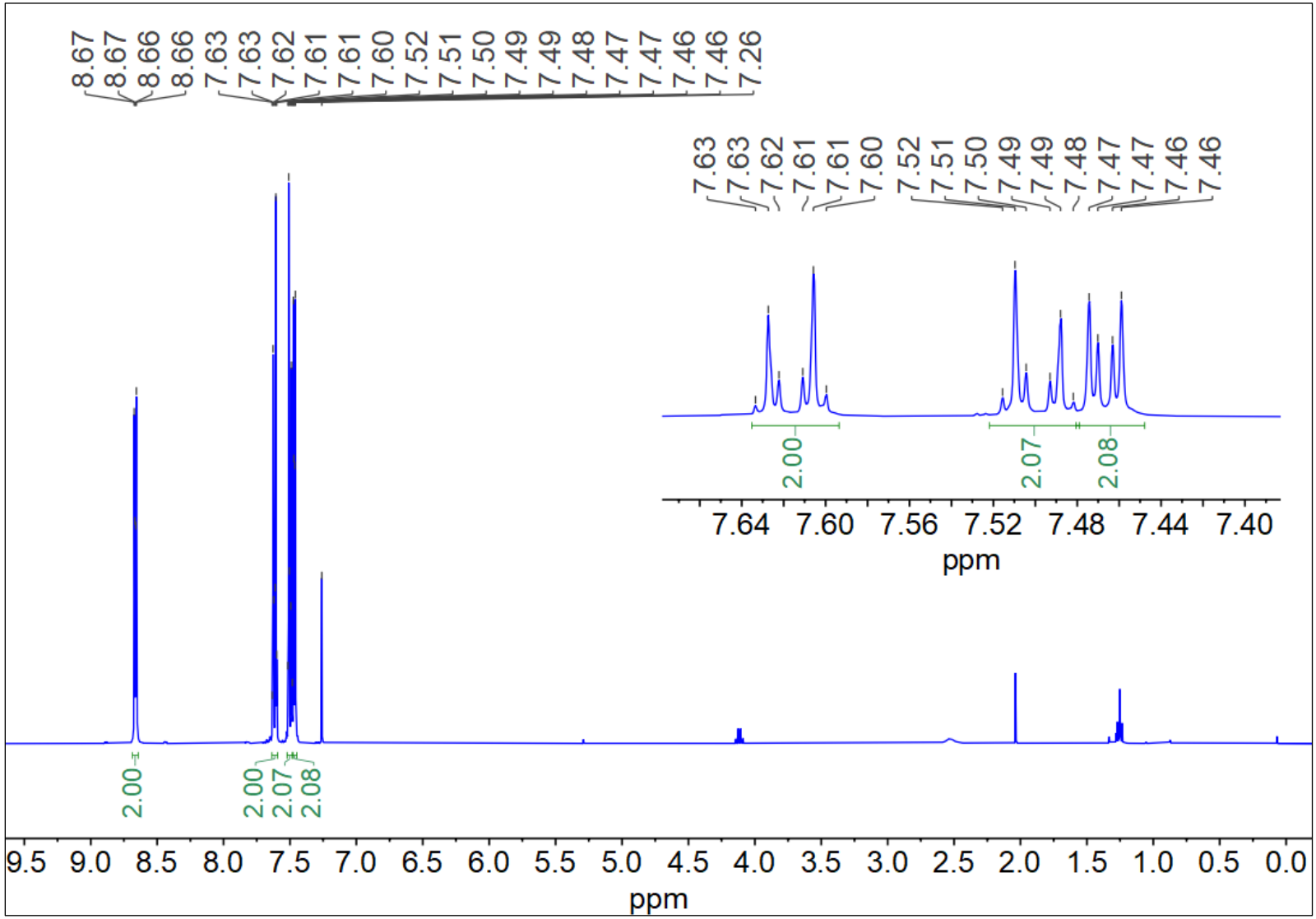

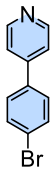

^{13}C {^{1}H} NMR (100 MHz, $CDCl_3$): 4-(4-Bromophenyl) pyridine (**6**)

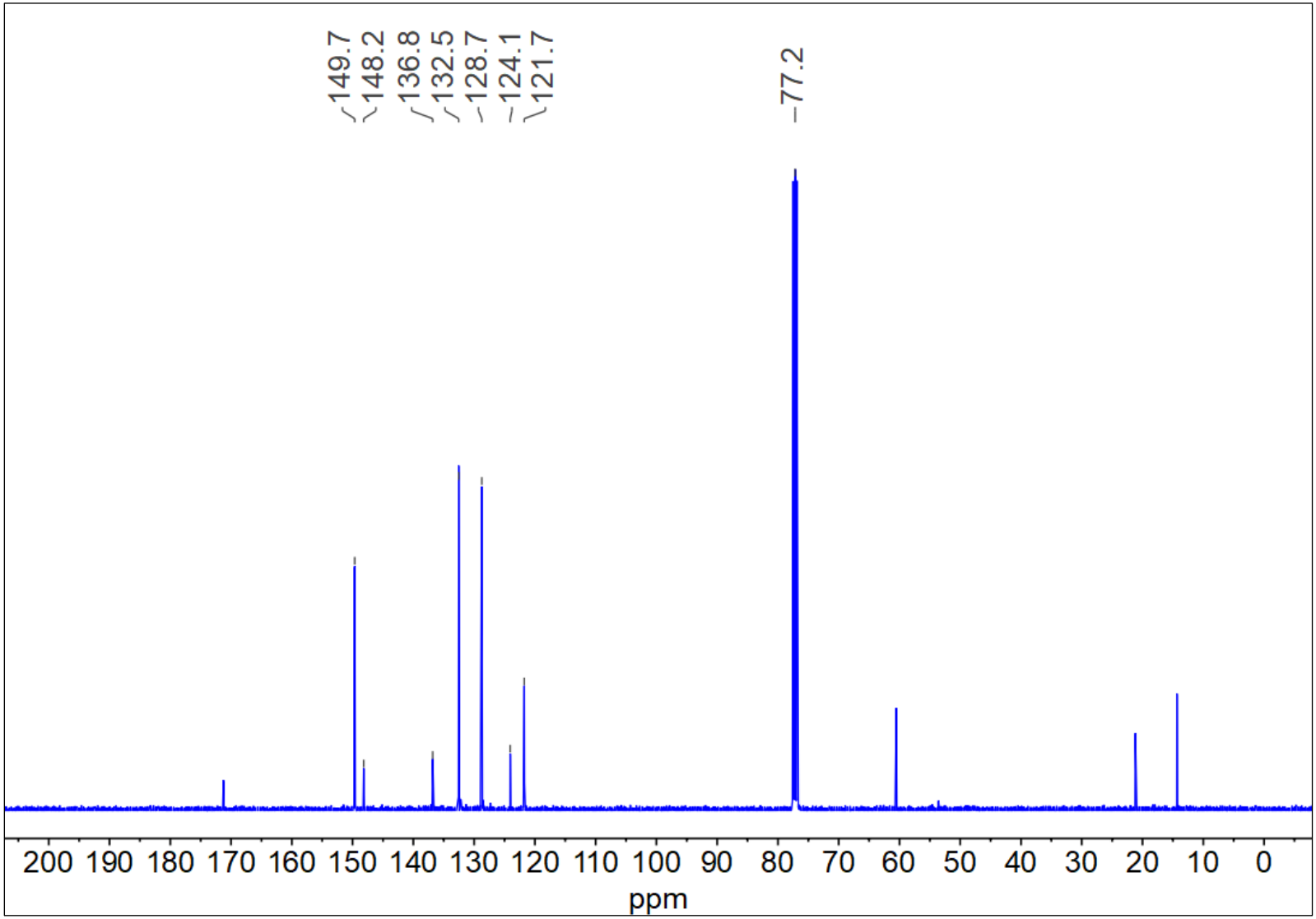

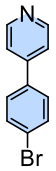

^{1}H – ^{1}H COSY ($CDCl_3$): 4-(4-Bromophenyl) pyridine (**6**)

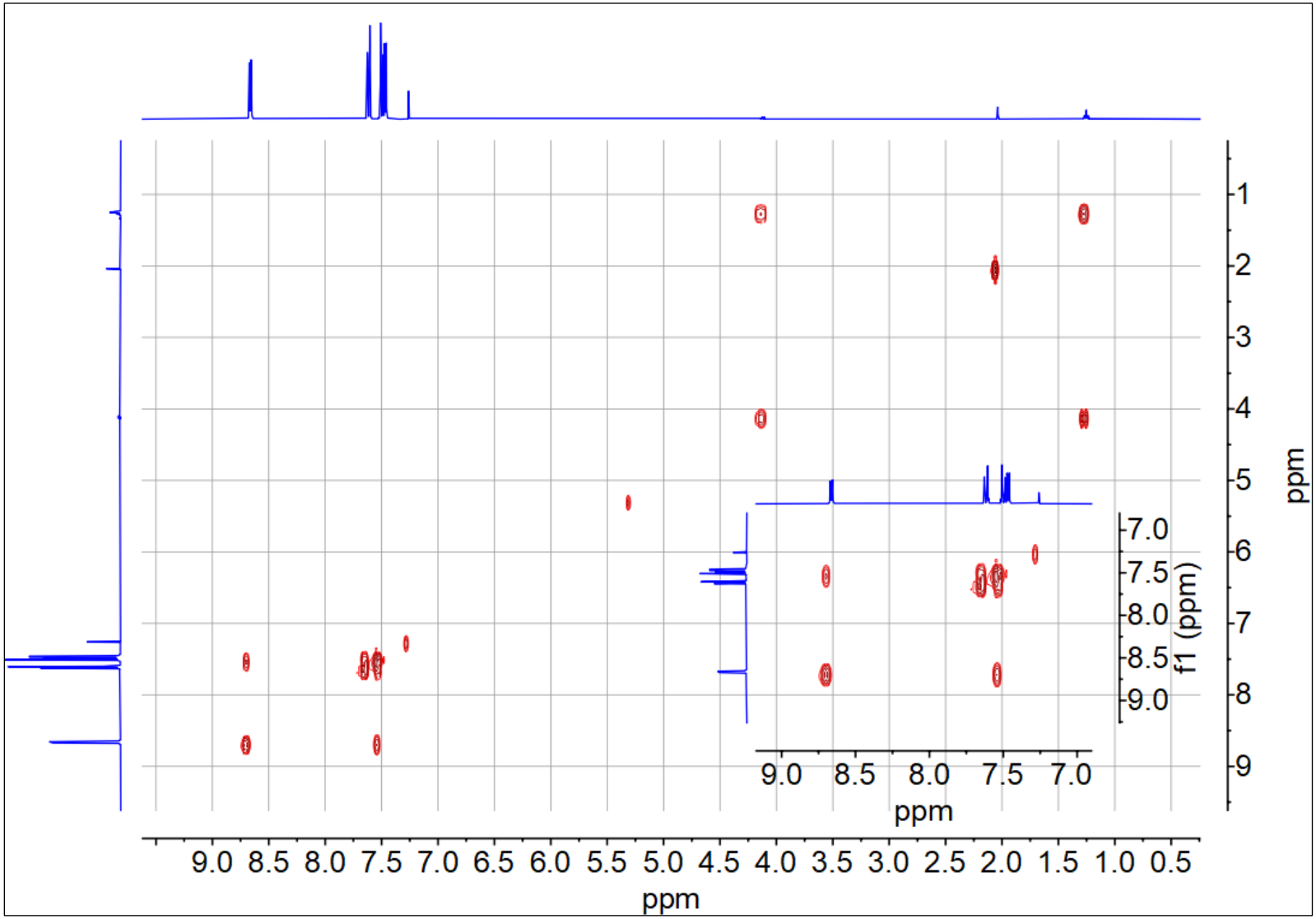

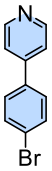

^{1}H – ^{13}C HSQC ($CDCl_3$): 4-(4-Bromophenyl) pyridine (**6**)

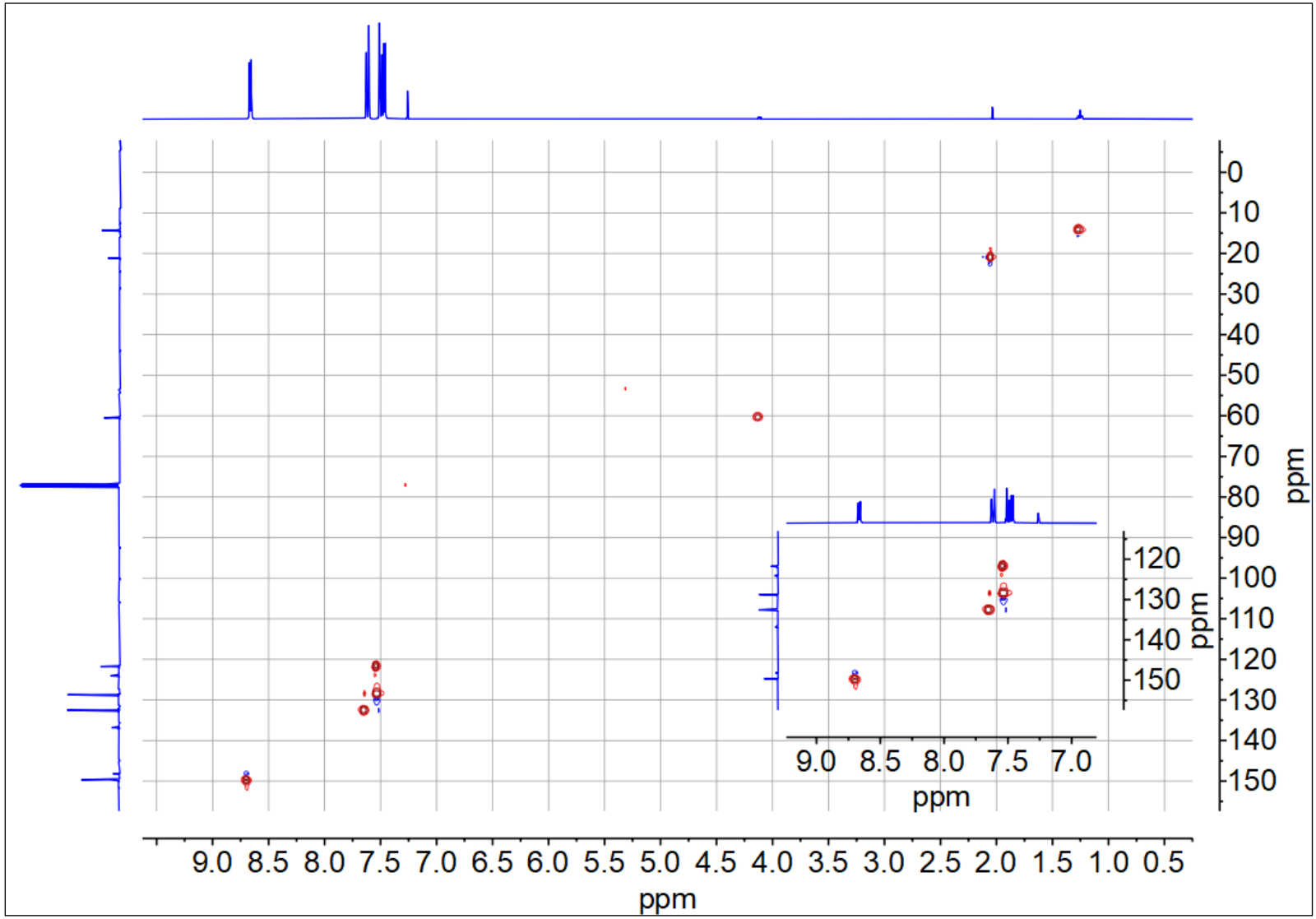

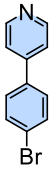

^{1}H – ^{13}C HMBC ($CDCl_3$): 4-(4-Bromophenyl) pyridine (**6**)

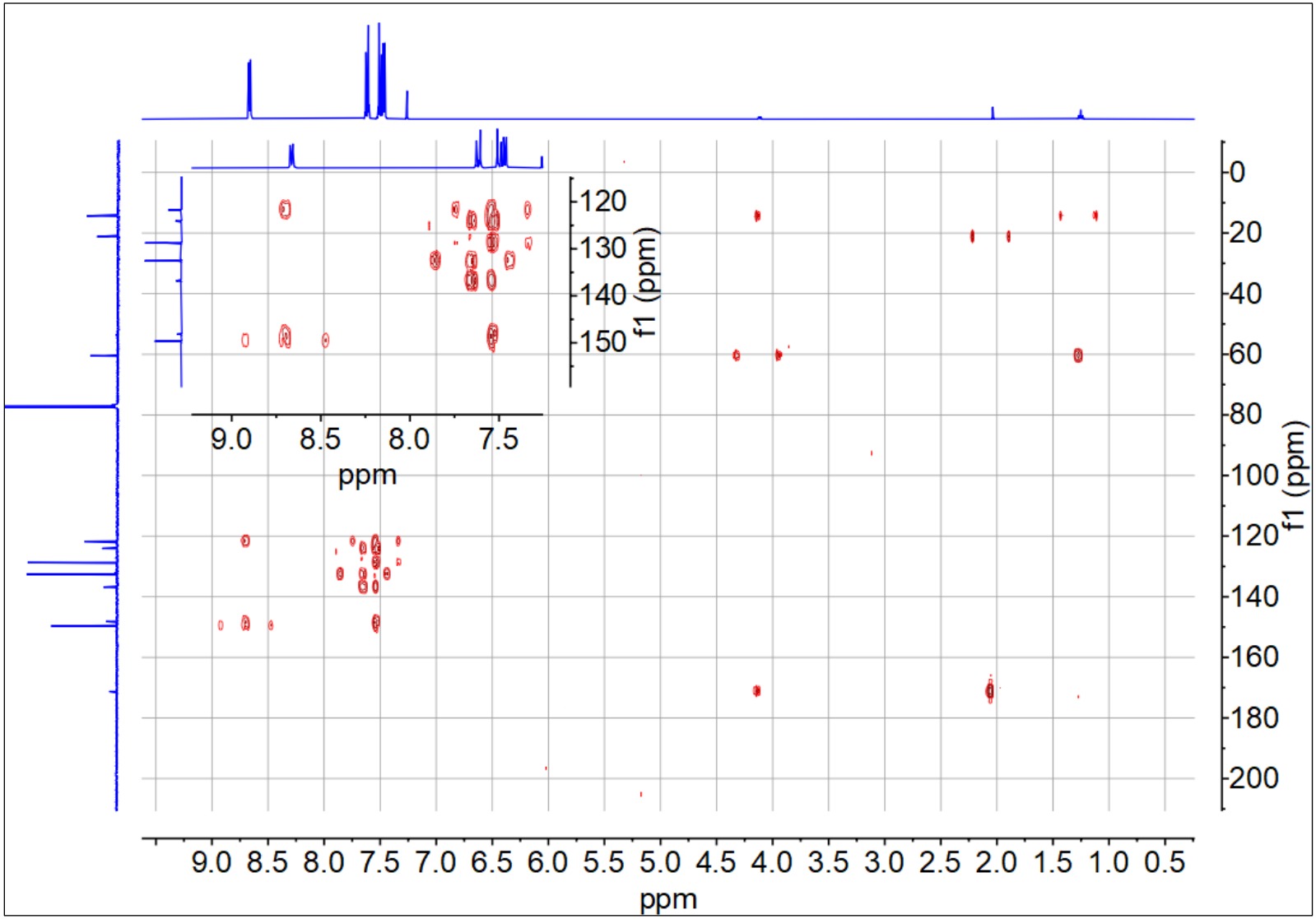

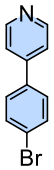

^{1}H NMR (400 MHz, $CDCl_3$): 4-(4-Bromophenyl)-1-(2,4-dinitrophenyl)pyridin-1-ium chloride (**8**)

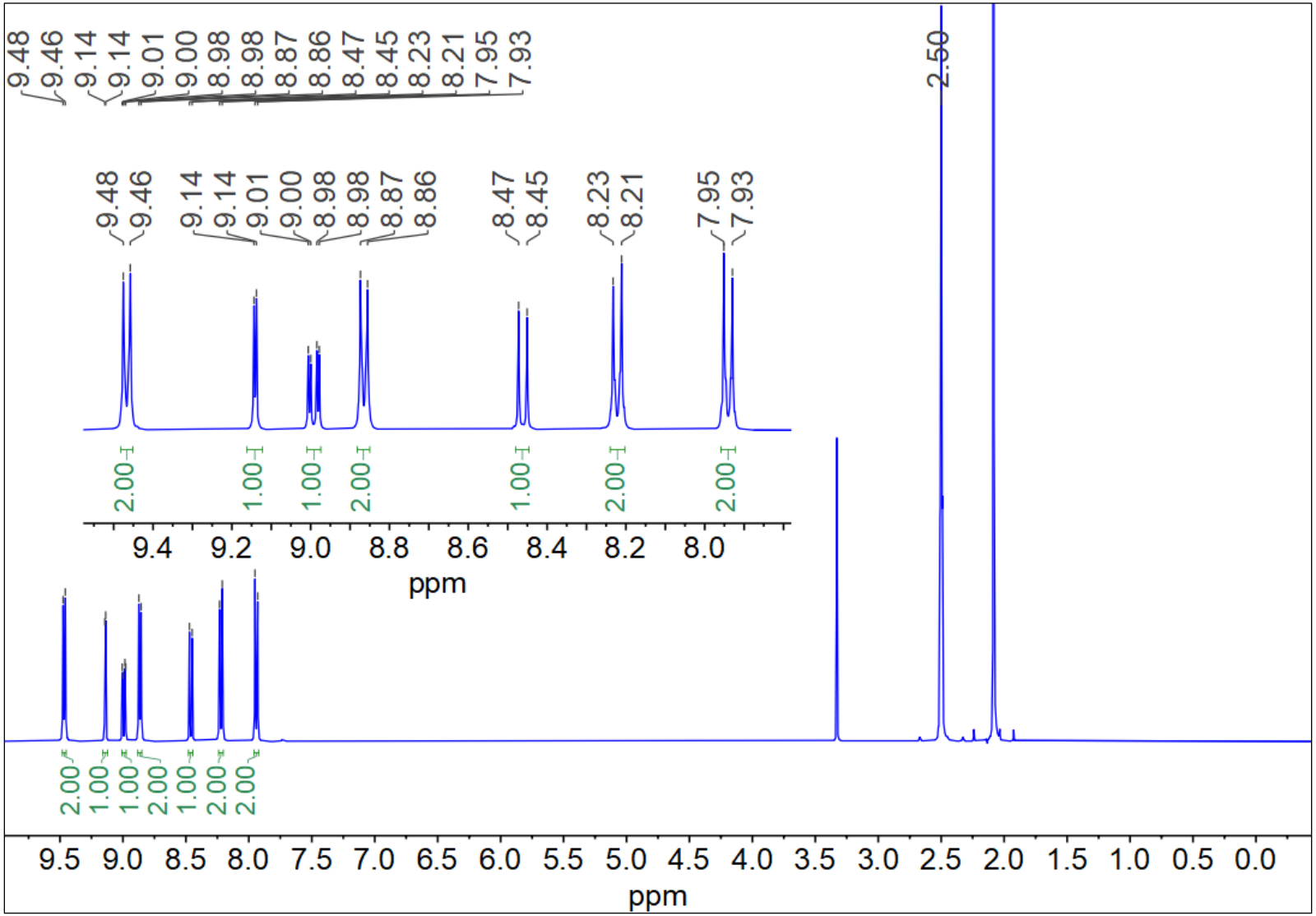

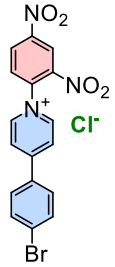

^{1}H NMR (400 MHz, $CDCl_3$): 4-(4-Bromophenyl)-1-(2,4-dinitrophenyl)pyridin-1-ium chloride (**8**)

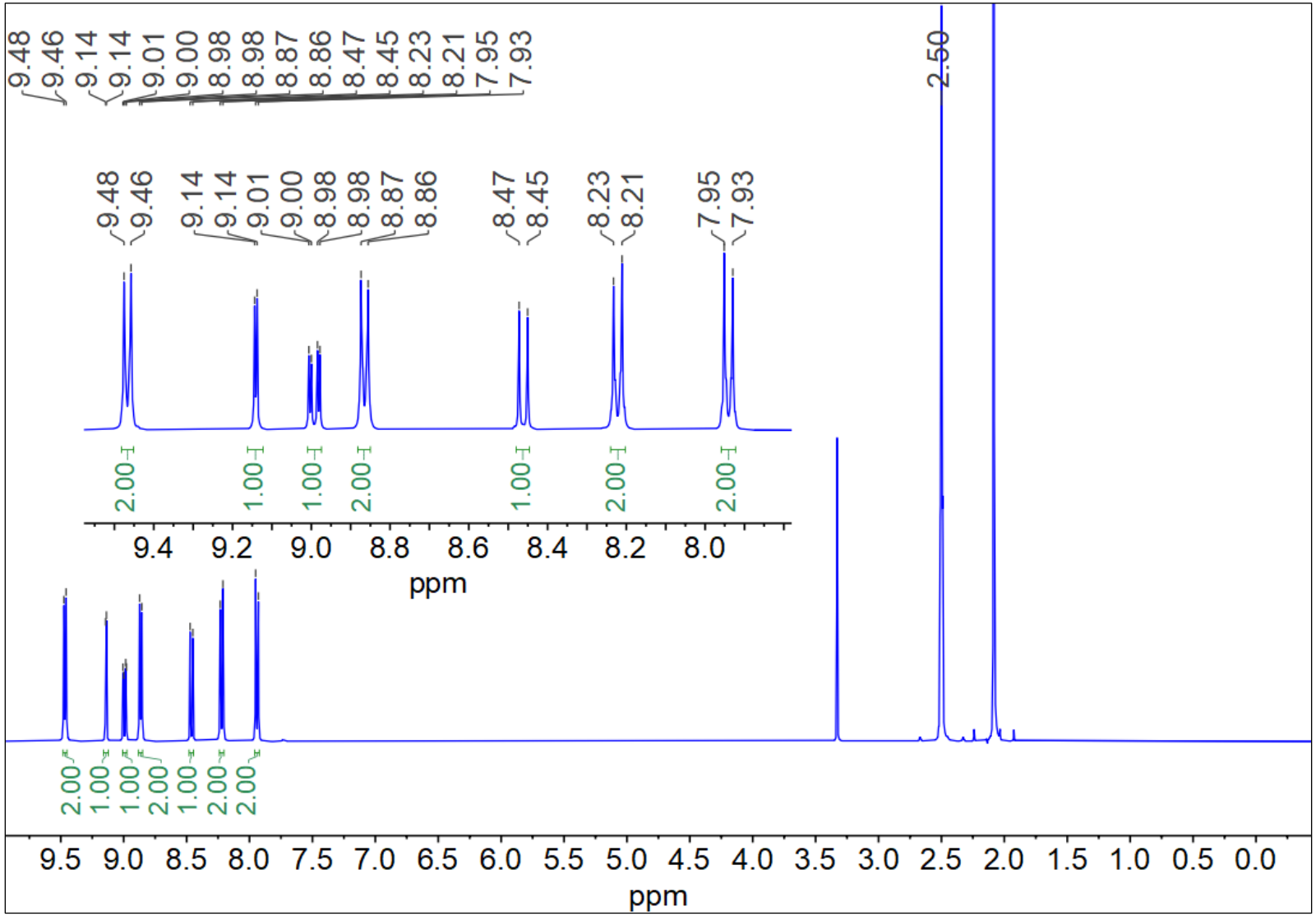

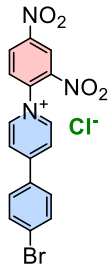

^{13}C {^{1}H} NMR (100 MHz, $CDCl_3$): 4-(4-Bromophenyl)-1-(2,4-dinitrophenyl)pyridin-1-ium chloride (**8**)

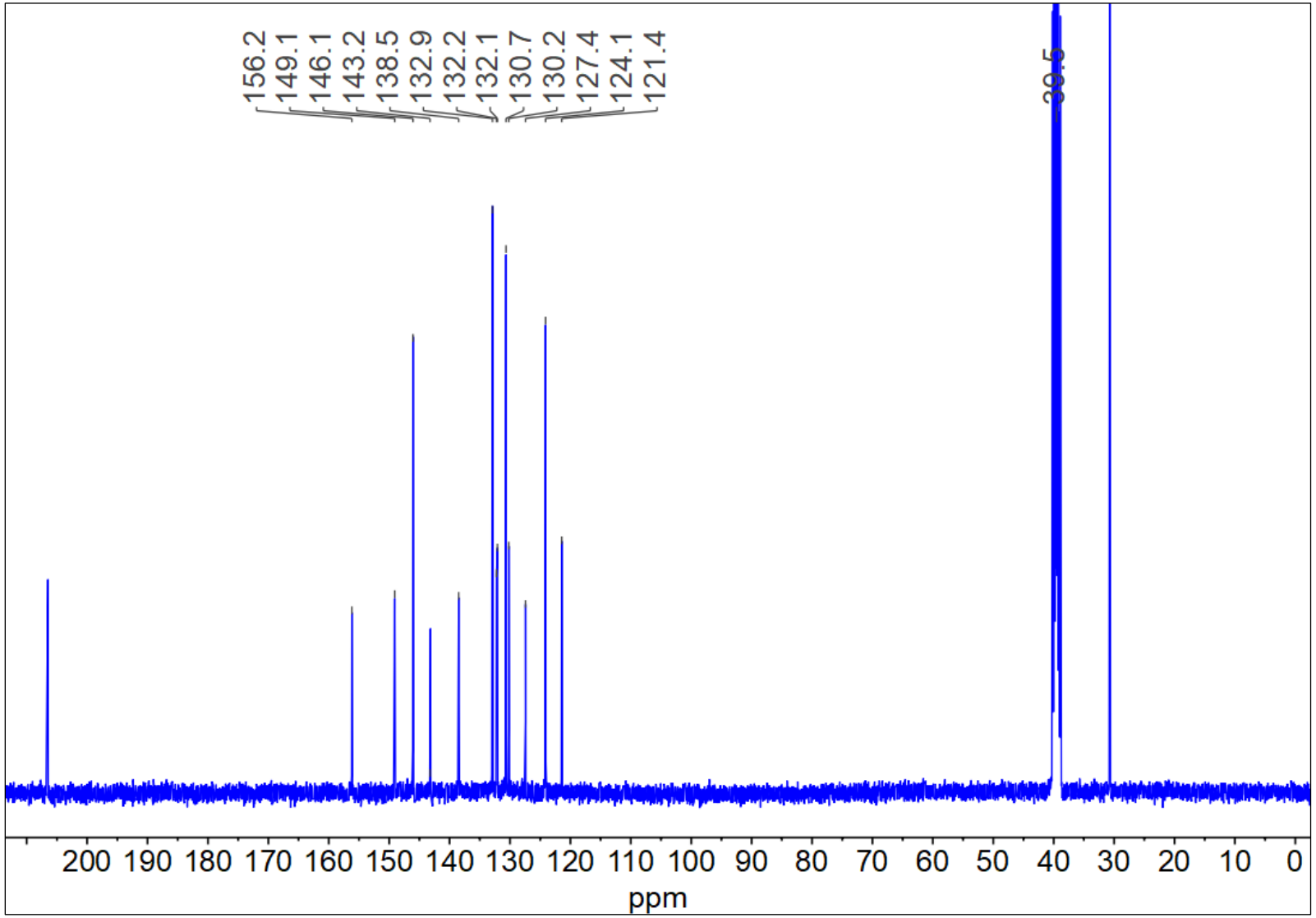

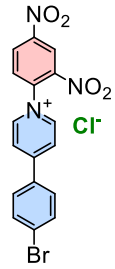

^{1}H – ^{1}H COSY ($CDCl_3$): 4-(4-Bromophenyl)-1-(2,4-dinitrophenyl)pyridin-1-ium chloride (**8**)

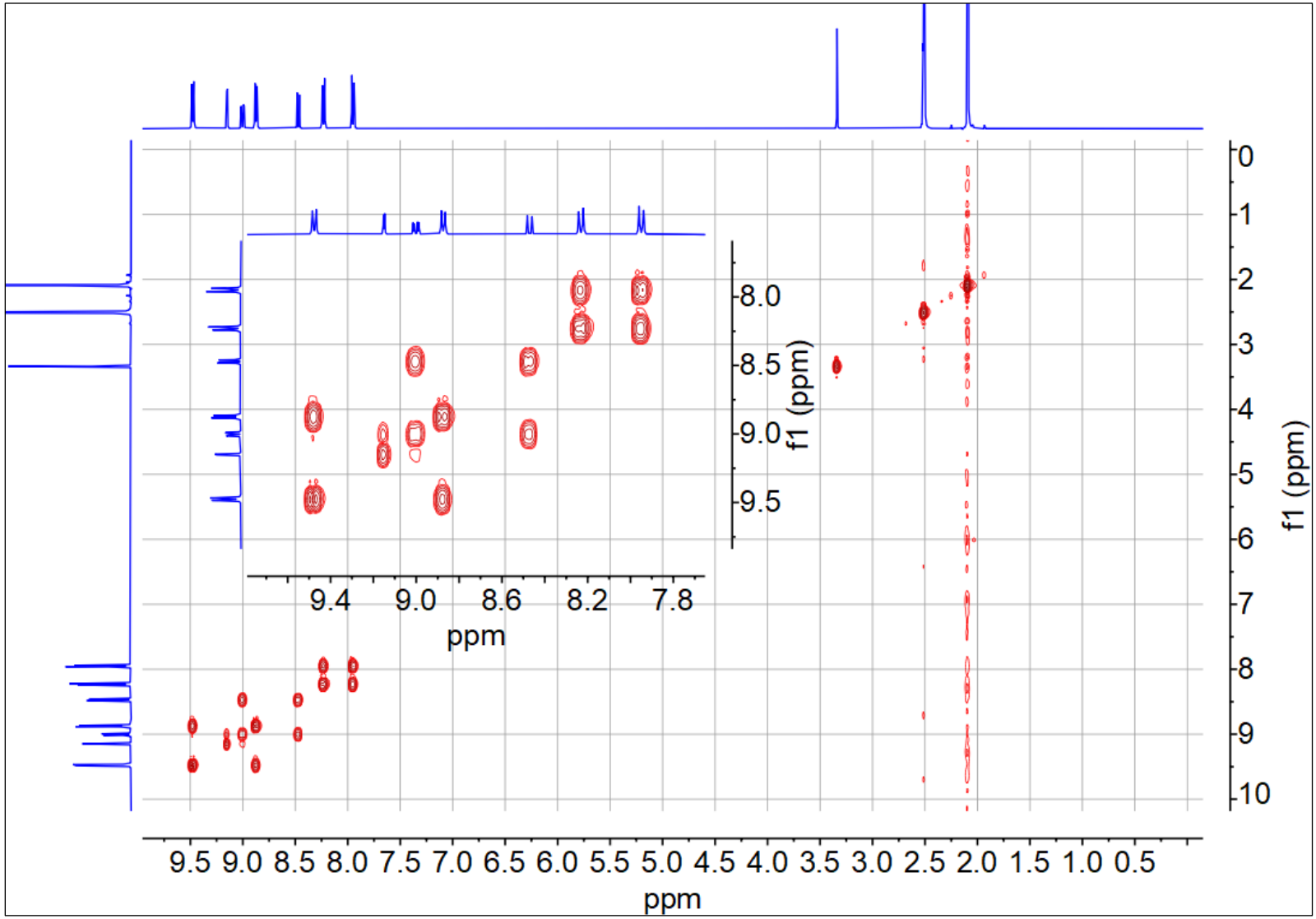

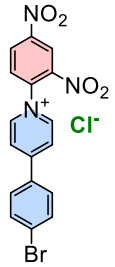

^{1}H – ^{13}C HSQC ($CDCl_3$): 4-(4-Bromophenyl)-1-(2,4-dinitrophenyl)pyridin-1-ium chloride (**8**)

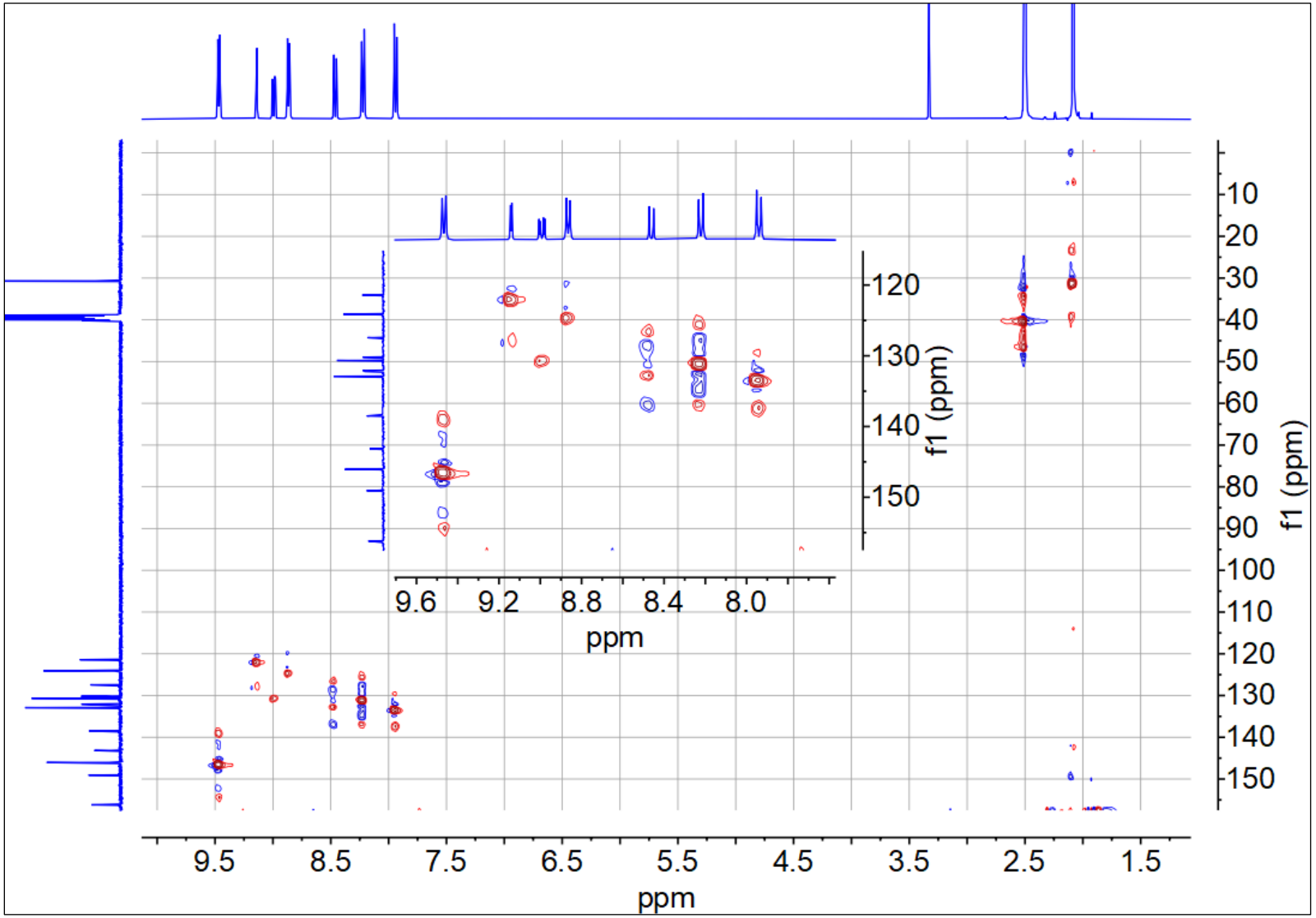

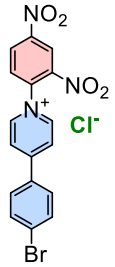

^{1}H – ^{13}C HMBC ($CDCl_3$): 4-(4-Bromophenyl)-1-(2,4-dinitrophenyl)pyridin-1-ium chloride (**8**)

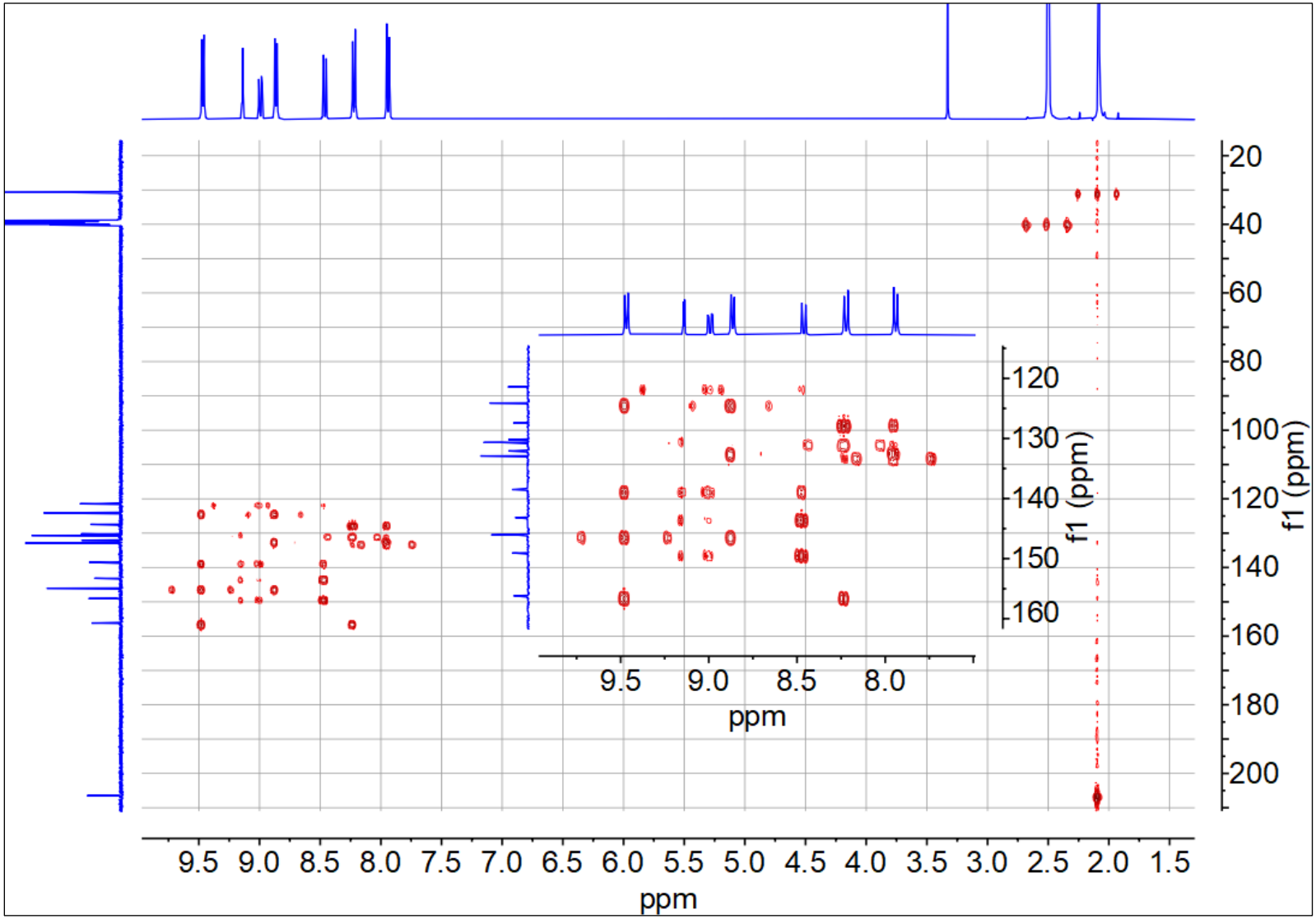

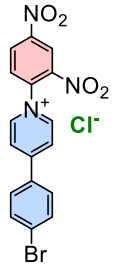

^{1}H NMR (400 MHz, acetonitrile-d_3):4-(4-Bromophenyl)-1-(1-adamantyl)pyridinium chloride (**10**)

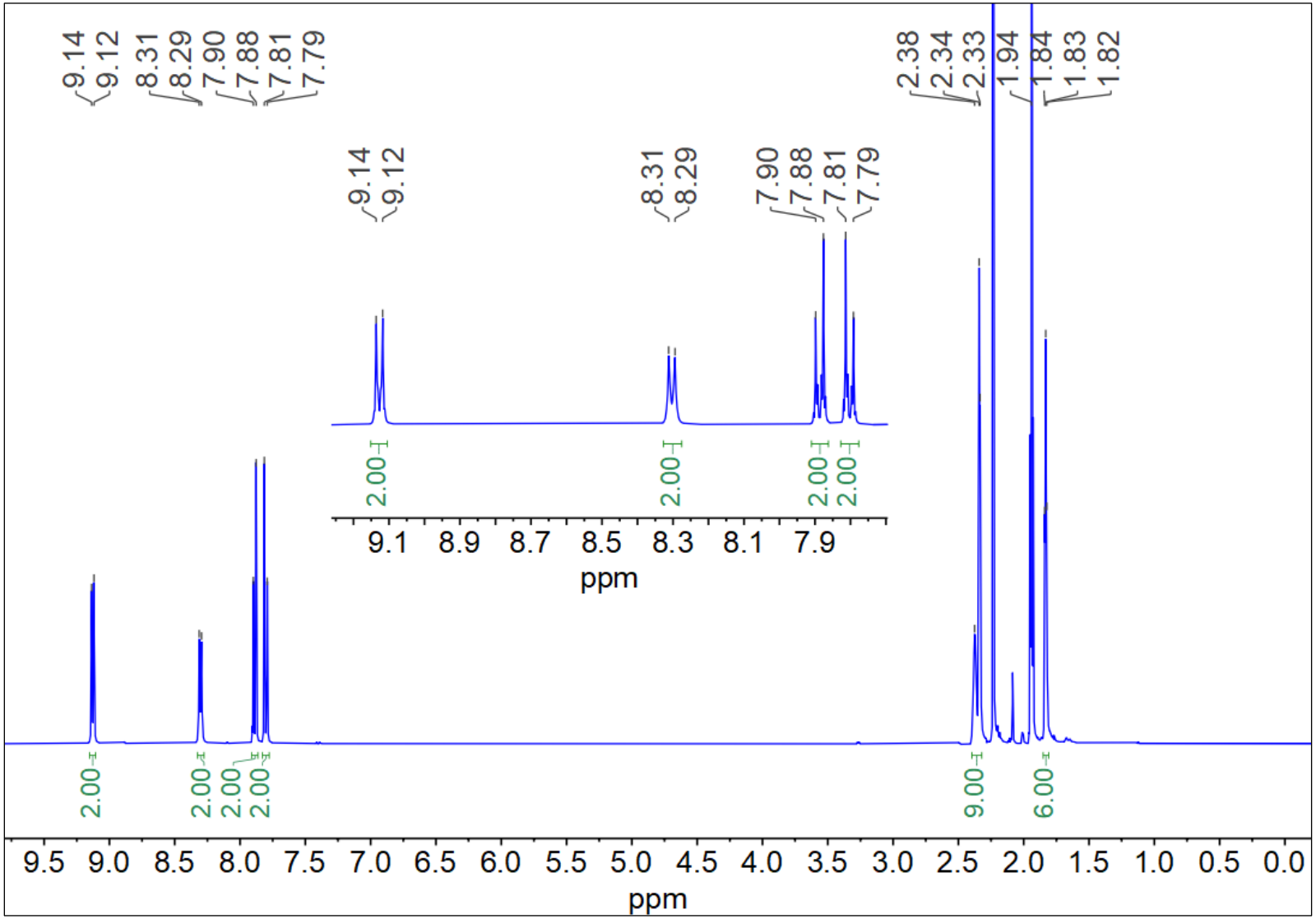

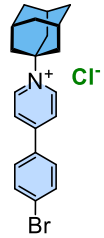

^{13}C {^{1}H} NMR (100 MHz, acetonitrile-d_3): 4-(4-Bromophenyl)-1-(1-adamantyl)pyridinium chloride (**10**)

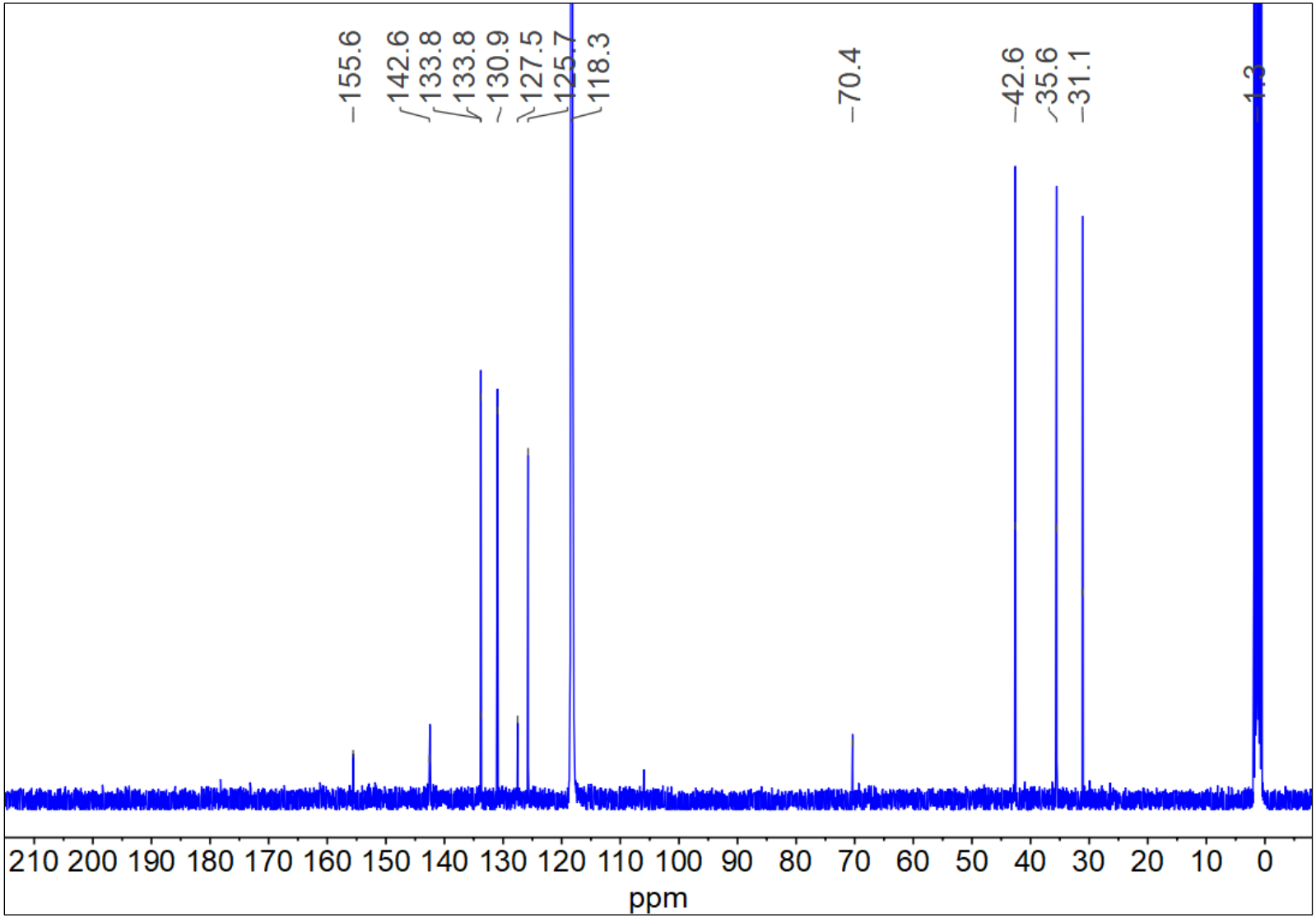

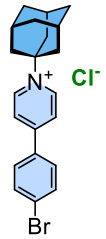

^{1}H – ^{1}H COSY (acetonitrile-d_3): 4-(4-Bromophenyl)-1-(1-adamantyl)pyridinium chloride (**10**)

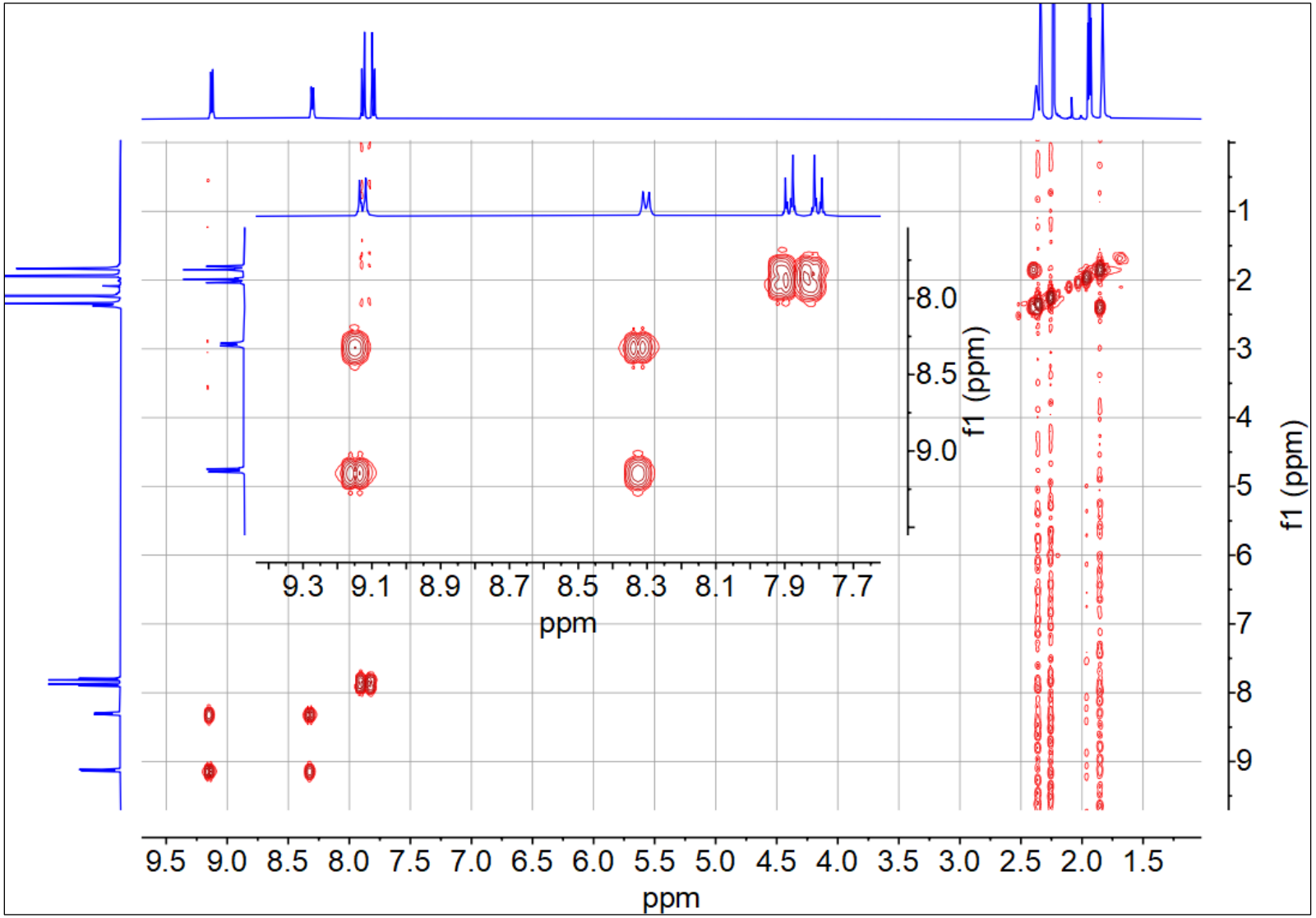

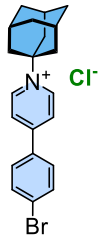

^{1}H – ^{13}C HSQC (acetonitrile-d_3): 4-(4-Bromophenyl)-1-(1-adamantyl)pyridinium chloride (**10**)

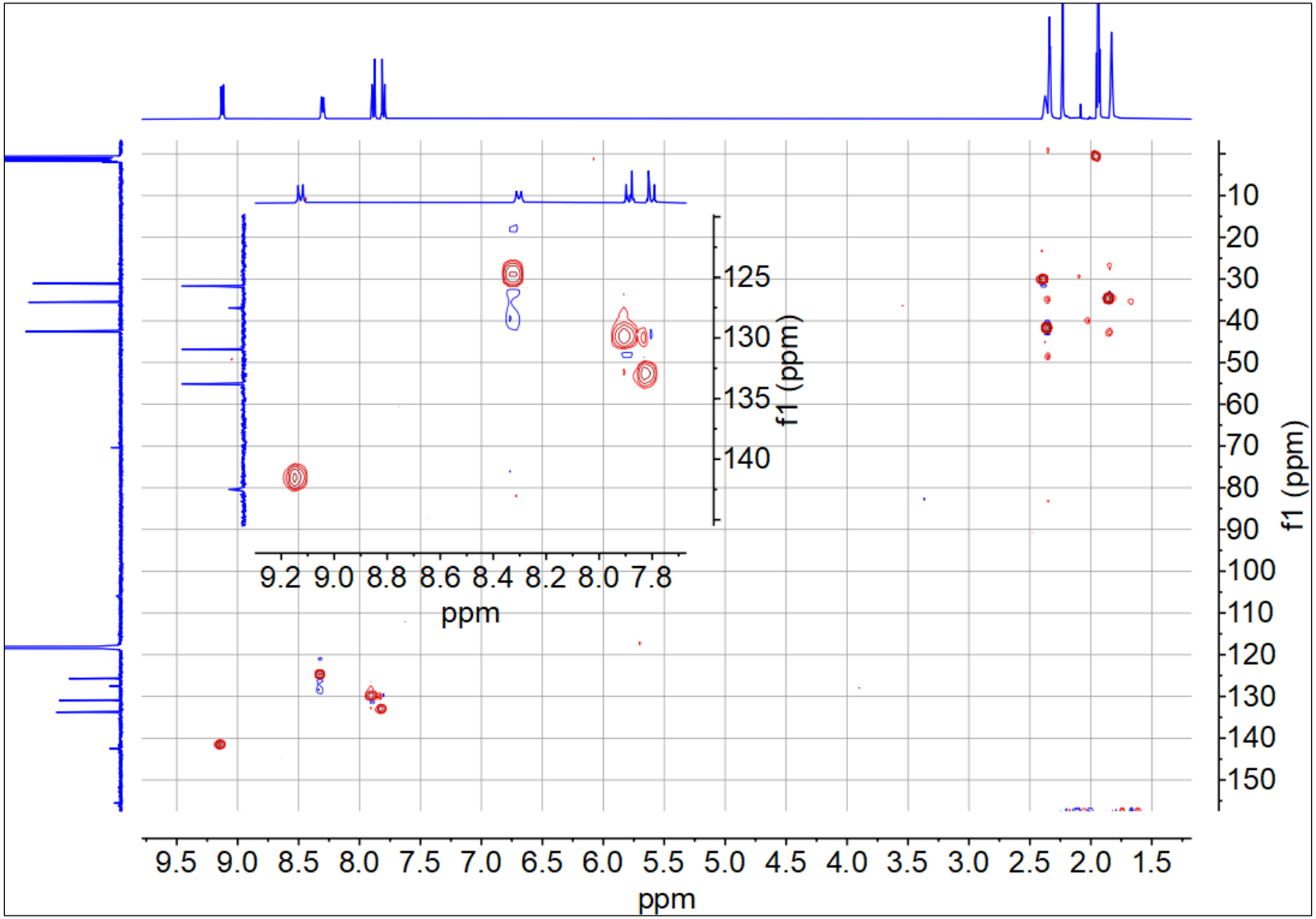

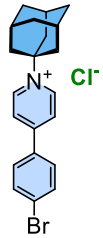

^{1}H – ^{13}C HMBC (acetonitrile-d_3): 4-(4-Bromophenyl)-1-(1-adamantyl)pyridinium chloride (**10**)

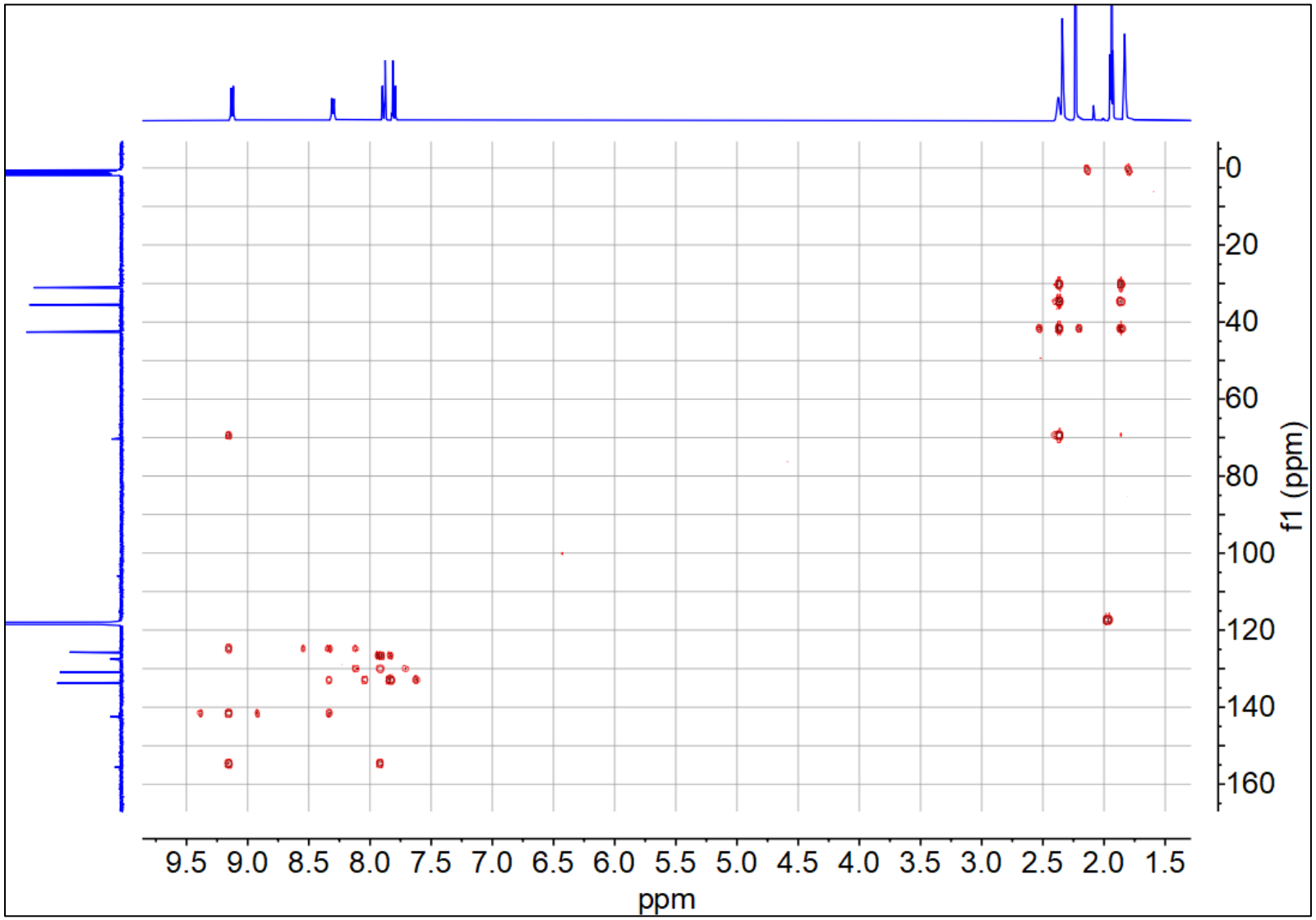

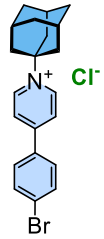

11. X-Ray Crystallographic Data

Table S1. Parameters of Single Crystals of **6**, **8** and **10**.

Compound	**6**	**8**	**10**
CCDC	2416417	2416418	2416416
Formula	$C_{11}H_8BrN$	$C_{17}H_{11}BrN_3O_4Cl\cdot1.236(H_2O)$	$C_{21}H_{23}BrNCl\cdot1.08(C_2H_4O)$
M.w.	234.09	458.92	452.45
Crystal system	Orthorhombic	Monoclinic	Monoclinic
Space group	*Fdd*2 (No.43)	*Cc* (No.9)	$P2_1/c$ (No.14)
a [Å]	17.1318 (6)	14.3576 (5)	7.2281 (3)
b [Å]	8.8789 (3)	42.1432 (15)	17.0092 (8)
c [Å]	12.0049 (4)	9.9596 (4)	16.9709 (7)
α [°]			
β [°]		114.105 (1)	96.963 (2)
γ [°]			
Z	8	12	4
V[Å^3]	1826.08 (11)	5500.8 (4)	2071.09 (16)
Temperature	120	120	120
D_x [g cm^{-3}]	1.703	1.662	1.451
Wavelength, Å	0.71073	0.71073	0.71073
Crystal size [mm]	0.21 × 0.13 × 0.07	0.18 × 0.16 × 0.10	0.23 × 0.09 × 0.06
Crystal color, shape	Irregular, colourless	Prism, yellow	Prism, colourless
μ [mm^{-1}]	4.45	2.42	2.13
T_{min},T_{max}	0.458, 0.746	0.664, 0.797	0.64, 0.884
Measured reflections	5773	130821	80731
Independent diffractions (R_{int}[a])	1336, (0.018)	12596, (0.035)	4751, (0.027)
Observed diffract. [I>2σ(I)]	1283	12292	4604
No. of parameters	62	759	217
R[b]	0.013	0.030	0.021
wR(F^2) for all data	0.034	0.084	0.054
GOF[c]	1.1	1.04	1.07
Residual electron density [e/Å^3]	0.32, -0.15	2.22, -0.84	0.50, -0.42
Absolute structure parameter	-0.009 (5)	-0.0014 (15)	

[a] $R_{int} = \Sigma \left| F_o^2 - F_{o,mean}^2 \right| / \Sigma F_o^2$; [b] $R(F) = \Sigma \left| \left| F_o \right| - \left| F_c \right| \right| / \Sigma \left| F_o \right|$; $wR(F^2) = [\Sigma(w(F_o^2 - F_c^2)^2)/(\Sigma w(F_o^2)^2)]^{½}$;
[c] $GOF = [\Sigma(w(F_o^2 - F_c^2)^2)/(N_{diffrs} - N_{params})]^{½}$

X-ray: 4-(4-Bromophenyl)pyridine (**6**) (displacement ellipsoids are shown at the 50% probability level)

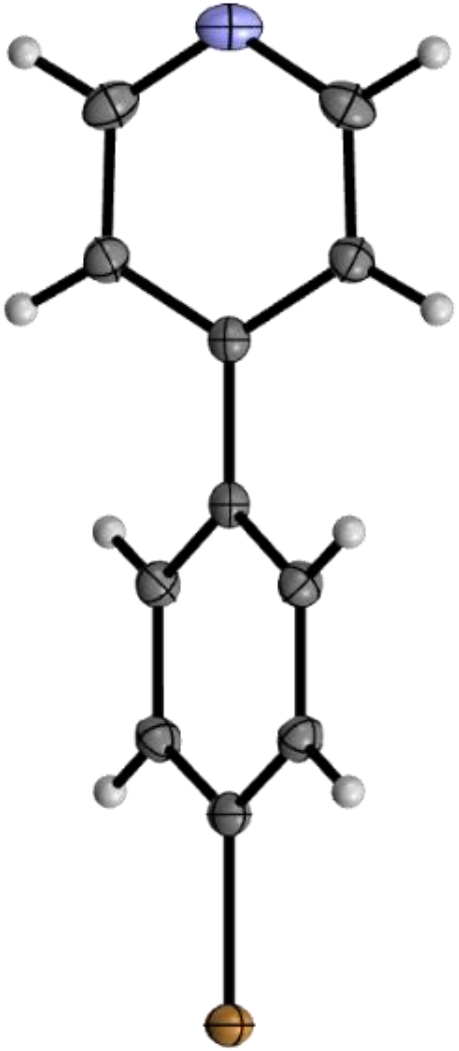

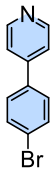

X-ray: Crystal packing of 4-(4-bromophenyl)pyridine (**6**) (Hydrogens are omitted for clarity)

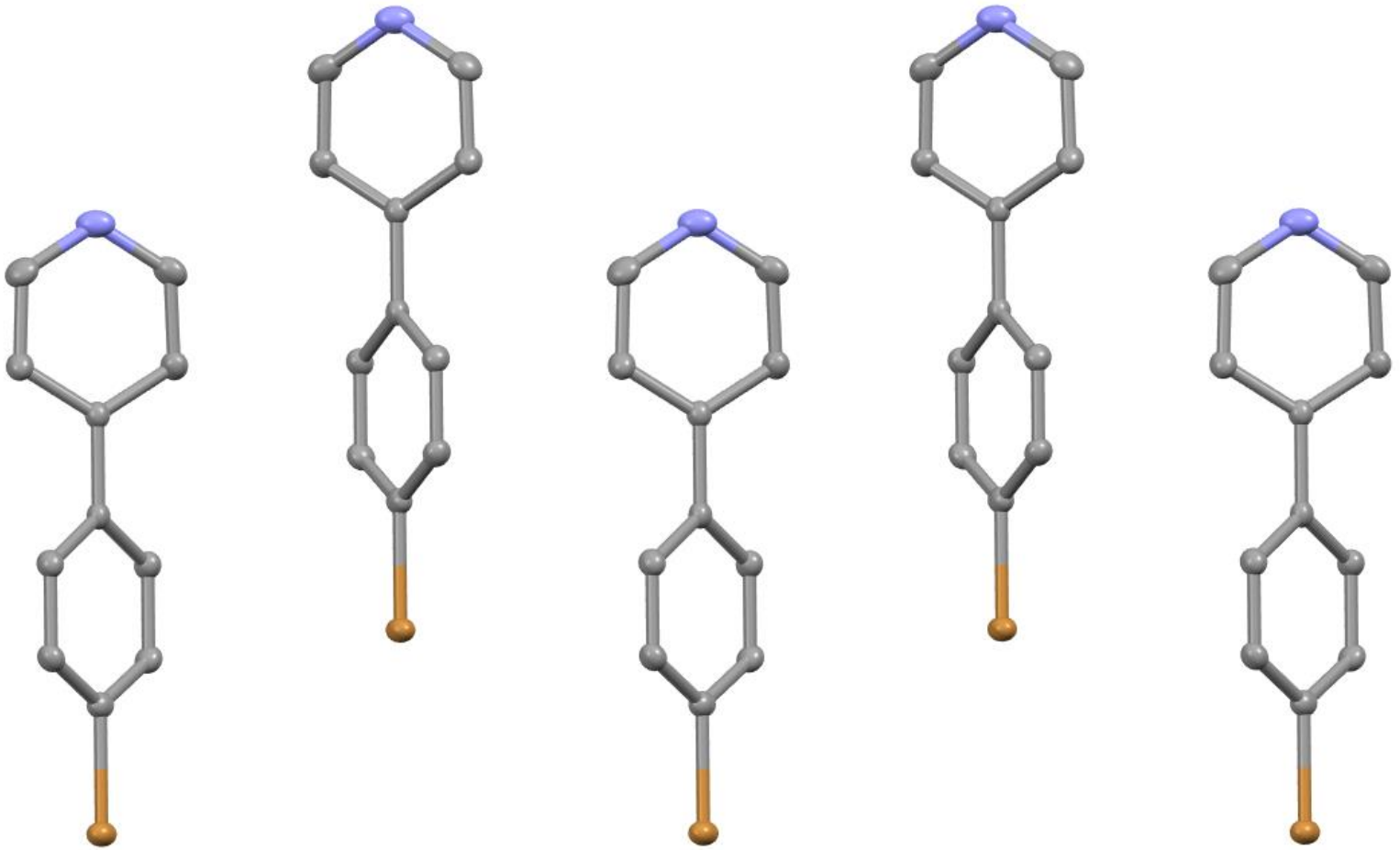

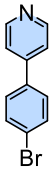

X-ray: 4-(4-Bromophenyl)-1-(2,4-dinitrophenyl)pyridin-1-ium chloride (**8**) (displacement ellipsoids are shown at the 50% probability level)

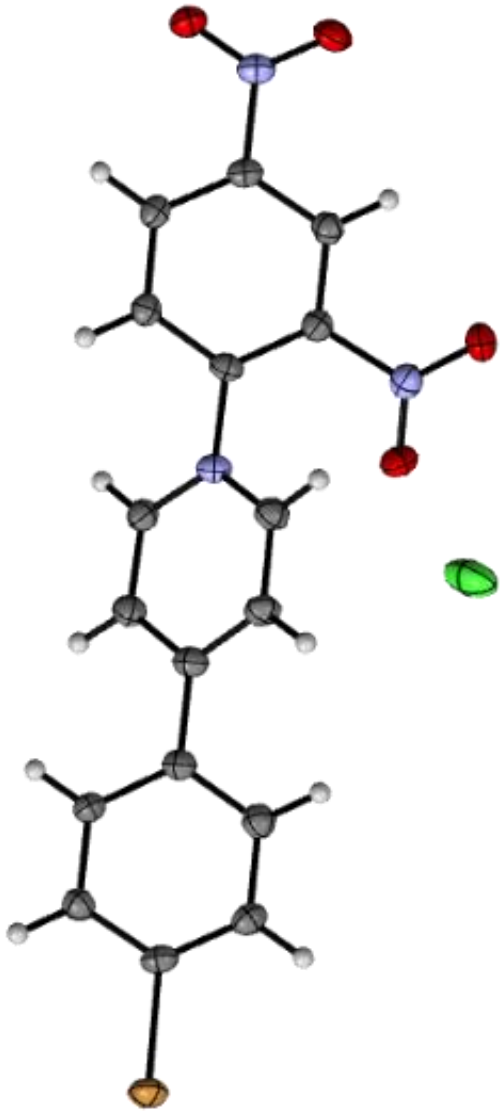

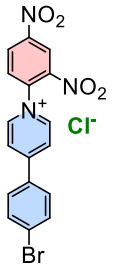

X-ray: Crystal packing of 4-(4-bromophenyl)-1-(2,4-dinitrophenyl)pyridin-1-ium chloride (**8**) (Hydrogens are omitted for clarity)

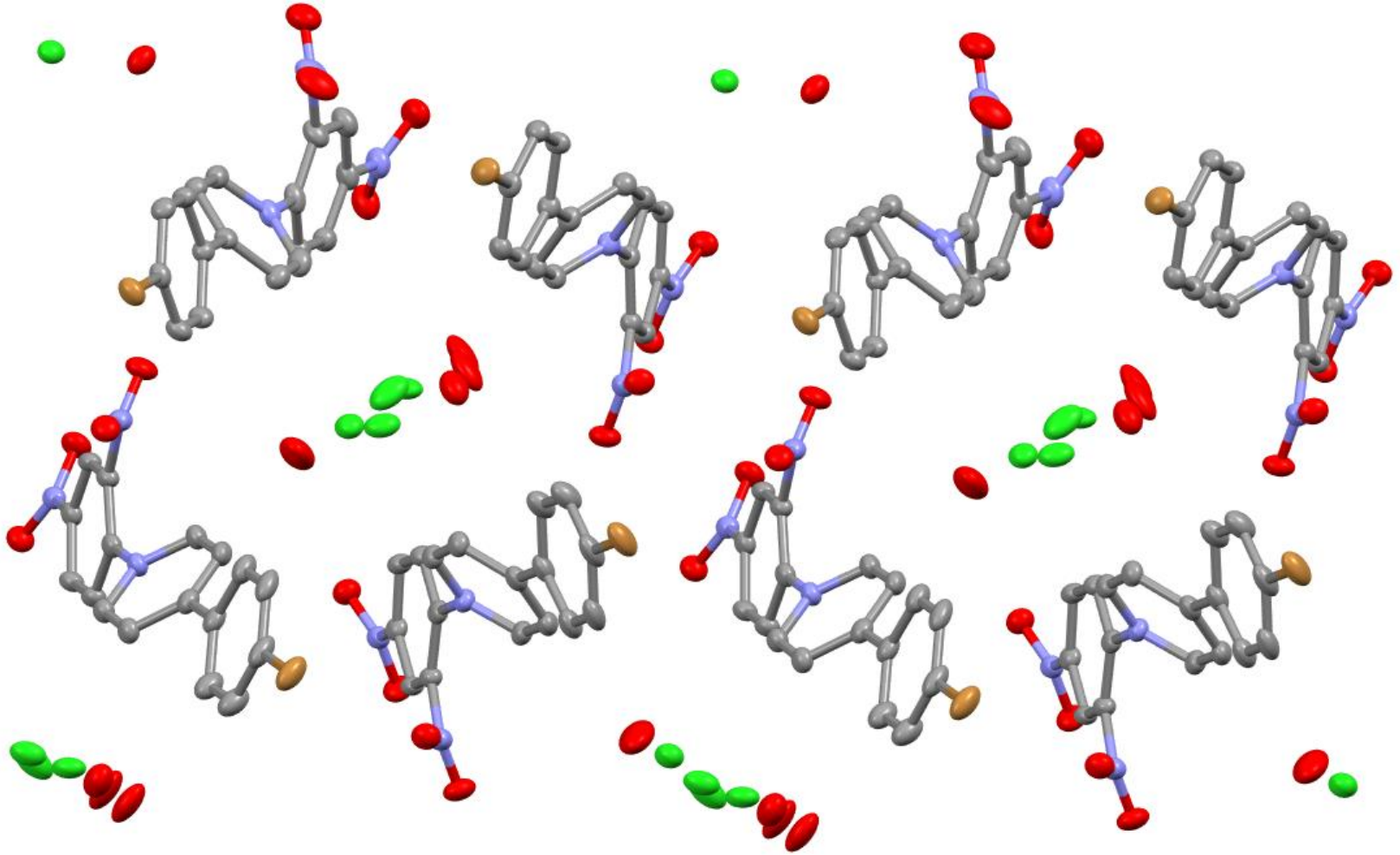

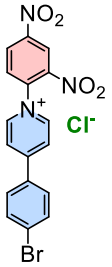

X-ray: Compound **10** (displacement ellipsoids are shown at the 50% probability level)

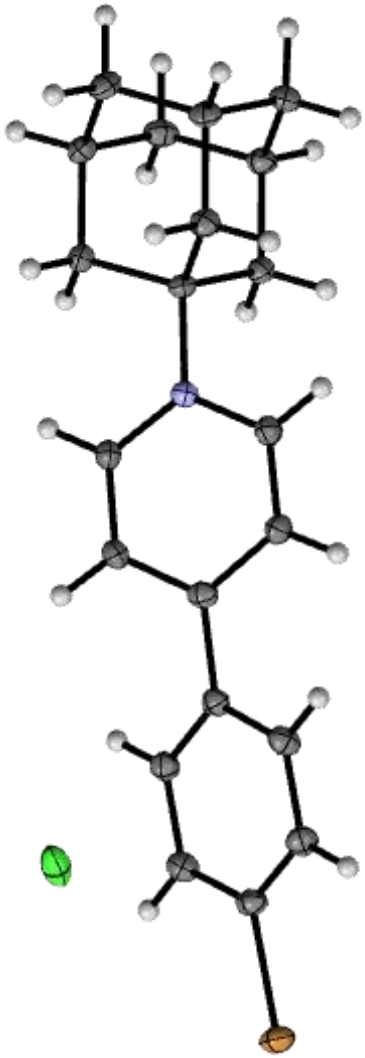

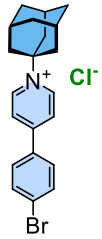

X-ray: Crystal packing of compound **10** (Hydrogens are omitted for clarity)